Review article

Hydrogel microparticles for biosensing

Gaelle C. Le Goff [a,b], Rathi L. Srinivas [b], W. Adam Hill [a], Patrick S. Doyle [b,*]

[a] Novartis Institutes for Biomedical Research, 250 Massachusetts Avenue, Cambridge, MA 02139, USA
[b] Department of Chemical Engineering, Massachusetts Institute of Technology, 77 Massachusetts Avenue, Cambridge, MA 02139, USA

ARTICLE INFO

ABSTRACT

Due to their hydrophilic, biocompatible, and highly tunable nature, hydrogel materials have attracted strong interest in the recent years for numerous biotechnological applications. In particular, their solution-like environment and non-fouling nature in complex biological samples render hydrogels as ideal substrates for biosensing applications. Hydrogel coatings, and later, gel dot surface microarrays, were successfully used in sensitive nucleic acid assays and immunoassays. More recently, new microfabrication techniques for synthesizing encoded particles from hydrogel materials have enabled the development of hydrogel-based suspension arrays. Lithography processes and droplet-based microfluidic techniques enable generation of libraries of particles with unique spectral or graphical codes, for multiplexed sensing in biological samples. In this review, we discuss the key questions arising when designing hydrogel particles dedicated to biosensing. How can the hydrogel material be engineered in order to tune its properties and immobilize bioprobes inside? What are the strategies to fabricate and encode gel particles, and how can particles be processed and decoded after the assay? Finally, we review the bioassays reported so far in the literature that have used hydrogel particle arrays and give an outlook of further developments of the field.

© 2015 Elsevier Ltd. All rights reserved.

Contents

* Corresponding author.
  E-mail address: pdoyle@mit.edu (P.S. Doyle).

1. Introduction

In recent years, there has been significant development of hydrogel-based technologies for a range of biotechnology applications including diagnostics [1–3], drug delivery [4,5], and tissue engineering [1,6–8]. Hydrogels are versatile materials due to their hydrophilic, biofriendly, and highly tunable nature, making them applicable in this varied range of contexts. Recent significant advances in types of gel materials [9,10], microfabrication techniques [11–14] and biosensor development [15] have come together to assemble the key components for fabrication of encoded hydrogel particles for biosensing. In this review, we will focus specifically on the development of these unique microparticles for biosensing, methods of synthesis and functionalization, and detection assays that have been reported in literature. We will also comment on the future of the field and the expansion into other areas such as single-cell characterization. This introduction will enumerate the chemical advantages of hydrogels and their initial success in being used in a microarray format, which led to the gel bead-based advances that we will describe later.

Hydrogels, made of cross-linked hydrophilic polymer chains, are readily functionalized with diverse biological entities such as nucleic acids or proteins [5]. Thus, hydrogels can be engineered for capture and detection of clinically relevant analytes including but not limited to proteins, DNA, mRNA, and microRNA (miRNA). Their solution-like environment, chemical tunability and non-fouling nature in biologically complex fluids (e.g. serum), further render hydrogels ideal candidates for diagnostic applications. The three-dimensional scaffold can be porosity-tuned to allow the diffusion and reaction of large biomolecules while remaining structurally stable under harsh mixing or flow conditions.

In a molecular diagnostic context, hydrogels were first utilized for the fabrication of hydrogel sensing planar microarrays (Fig. 1). A wide range of hydrogel chemical compositions have been explored for DNA or protein microarrays, in particular polyacrylamide [2,16,17], polyethylene glycol [18–20], and alginate [21] derivatives. Several methods to functionalize the gels have been explored, ranging from in situ functionalization at the time of synthesis to post-synthesis functionalization utilizing functional groups in the gel [22]. In a series of studies where probe-functionalized polyacrylamide hydrogel pads were immobilized on a surface for DNA detection, hydrogels were found to be superior for biosensing relative to rigid two-dimensional planar surfaces [22–25]. These pioneering studies demonstrated better thermodynamic association constants for nucleic acid hybridization inside the gel environment and proved that biological probes could be functionalized at significantly higher densities than possible on standard microarrays. Further studies extended to antibody-based protein detection revealed similar advantages with regard to probe-functionalization density [2,26]. These favorable characteristics enabled
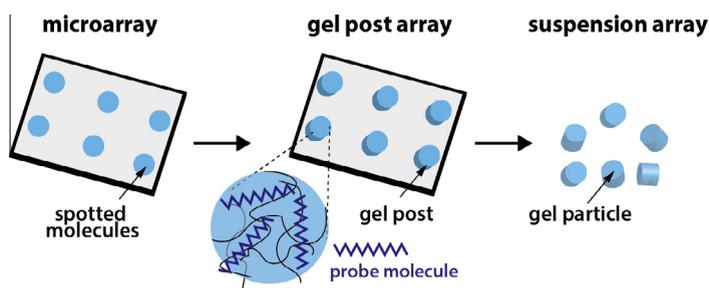
Fig. 1. From microarrays to gel particle arrays. Cartoon depiction of technology advancements that led to creation of hydrogel particle arrays. Spots on microarrays were first translated into hydrogel spots functionalized with biological probes. Techniques were then established to fabricate free-floating hydrogel particles that were similarly functionalized and could be suspended in solution for assays.

higher specificity and detection sensitivity inside the gel environment. We note that the substrate used in those studies, polyacrylamide, has a small pore size ($\sim$ nm) and analytes showed significantly hindered diffusion inside the gels [27]. Despite this constraint, the gel microarrays had significant advantages over planar microarrays simply due to the unique chemistry inside the gel environment.

Most planar microarrays, however, suffer from inherent diffusional limitations that are difficult to overcome since these systems are not well mixed. These constraints apply to hydrogel planar arrays as well. For example, assuming solution diffusivity of a protein to be $\sim$100 μm^2/s [28], the characteristic diffusion time across even 1 cm is on the order of days. This precludes the possibility of reaching equilibrium in a reasonable period of time. In addition, although microarrays can accommodate high-density multiplexing, there is low flexibility with regards to rapidly changing probe sets to tailor clinical panels, since probes are pre-immobilized on a single surface. Instead, bead-based suspension arrays can overcome mass transfer limitations by maintaining a well-mixed solution through shaking, thereby providing near-solution kinetics, and further offering high flexibility for rapid target panel modification [29]. A natural advance in the field was thus to adapt hydrogel substrates in a particle-array format for solution-based detection.

In the field of particle-based arrays, the vast majority of reported examples focus on polyethylene glycol derived-materials, while a few recent studies use alginate gels. After discussing the properties of those materials and the strategies for probe immobilization (Section 2), we will review the methods for particle synthesis and encoding developed for these gels, ranging from graphical codes to spectral codes (Section 3). Among the key contributions to the field that we will discuss in this article are novel methodologies to fabricate multifunctional hydrogel microparticles using lithographic processes (including replica molding and stop flow lithography) [3] and spherical particles using droplet-based processes [13,30,31]. In some applications, gels were synthesized, functionalized and encoded in a single step, while in others synthesis, encoding and functionalization occurred at different times. We will review protocols for processing and reading the hydrogel particle array (Section 4) and examples of application for measurements of proteins, DNA, mRNAs and

microRNA, in a range of sensing conditions (Section 5). Finally, we will discuss the perspectives of hydrogel-based particle sensing, in particular how more recent assays have begun to examine the utility of such microparticles in applications such as single-cell analysis (Section 6).

2. Selecting a material and a strategy for probe immobilization

2.1. Materials

2.1.1. Polyethylene glycol

Polyethylene glycols (PEG) are commonly used in biotechnological applications due to their biocompatibility and low-biofouling properties [1,4–7]. In particular, PEG layers have been used to prevent non-specific binding of protein on sensing surfaces [19,32]. PEGs are relatively inexpensive and available in a large range of molecular weights and chemical modifications: PEG molecular weights ranging from a few hundred to several thousand grams per mole have been used to fabricate particles (Table 1). Conveniently, PEGs show good solubility in aqueous buffers required for biomolecule manipulation. PEG particles have thus been the substrate of choice for hydrogel particle-based assays so far (Table 2).

2.1.1.1. Polymerization reaction.
PEG particles are usually prepared using the free-radical polymerization of reactive (meth)acrylate PEG derivatives or polyethylene glycol diacrylates (PEGDA) (Fig. 2a) in the presence of a UV-sensitive photoinitiator, typically a hydroxyalkylphenone species (Table 1) [33–40]. The UV-induced activation of the photoinitiator generates a benzoyl free radical through a homolytic scission of a C–C bond, subsequently triggering the covalent crosslinking of the gel [41]. The controlled initiation and relatively fast propagation kinetics of this polymerization reaction are well suited to lithographic synthesis methods, as it will be further described in Section 3.2 [3].

2.1.1.2. Optimizing gel properties.
Different biosensing applications require the ability to fine-tune gel microstructure on-demand. Robust biomolecule capture and target accessibility should be ensured while maintaining

Table 1
Strategies for particle encoding and corresponding synthesis techniques.

Encoding strategies		Synthesis technique	Hydrogel material	Pre-polymer composition[a]	Biomolecule immobilization if reported	Refs.
Anisotropic graphical code	Shape	• Contact photolithography • UV crosslinked (365 nm)	PEG	PEGDA700 25% v/v, Darocur1173 2%, aqueous buffer with probe 73%	• Methacrylated oligonucleotide (covalent) • During synthesis	[33]
			PEG	PEGDA700 25% v/v, Darocur1173 1%, aqueous buffer with probe 74%	• Bacteria (physical entrapment) • During synthesis	[33]
	Shape	• Contact photolithography • UV crosslinked (365 nm)	PEG	PEGDA3400 or 8000, DMPA 1.5 mg/ml, enzyme 1 mg/ml	• Enzyme (physical entrapment) • During synthesis	[67]
			PEG	1:1 dilution of PEGDA700 in PBS, HOMPP 1%, functionalized magnetic nanoparticles (NP)	• Magnetic NP functionalized with enzyme (encapsulation) • During synthesis	[36]
			PEG	PEGDA575 50% v/v, acrylic acid 25% v/v, HOMPP 2%, aqueous buffer	• Protein (covalent; EDC/NHS-mediated reaction) • Post synthesis	[74]
	Shape	• Replica molding using soft lithography • UV crosslinked (365 nm)	PEG	Varying ratio of PEGDA700, PEG200, Darocur1173 and aqueous buffer with probe	• Acrylated oligonucleotide (covalent) • During synthesis	[37]
			PEG-chitosan hybrid	PEGDA700 30–48% v/v, chitosan oligomer 0–1.2% w/v, Darocur1173 2% v/v, water	• Functionalized oligonucleotide (covalent, Cu-free click chemistry reaction) • Post synthesis	[48]
	Bit-code (extruded holes)	• Stop-flow projection lithography • UV crosslinked (365 nm)	PEG	Varying ratio of PEGDA700, PEG200 or 600, Darocur1173 and aqueous buffer with probe or fluorescent dye	• Acrylated oligonucleotide (covalent) • During synthesis	[35,45,70,71,92]
			PEG	PEGDA700 18% v/v, PEG200 36% v/v, Darocur1173 4.5% v/v, aqueous buffer with probe 41.5% v/v	• Acrylated antibody (covalent) • During synthesis	[51,72]
Graphical and spectral encoding	Shape and structural color	• Contact photolithography • UV crosslinked (365 nm)	PEG-acrylamide	• 1st polymerization: PEGDA700 10% v/v, HMPPO 1% v/v, colloid crystal array in aqueous buffer • 2nd polymerization: acrylamide/bisacrylamide (29:1) 10% w/v, APS 1% w/v, TEMED 0.1% v/v, probe in aqueous buffer	• Acryl-modified oligonucleotide (covalent, copolymerization of a second gel layer on particle) • Post synthesis	[50]
	Bit-code and structural color	• Flow projection lithography using dynamic masking • UV crosslinked (365 nm)	PEG	• Code: superparamagnetic colloidal nanocrystal clusters dispersed in PEGDA700 75% v/v, water 25% v/v, DMPA 10 wt.% • Probe: PEGDA700 75% v/v, aqueous buffer with probe 25%, DMPA 10 wt.%	• Acrylated oligonucleotide (covalent) • During synthesis	[38]
Spectral encoding	Down-converting nanocrystals	• Droplet synthesis: herringbone mixer with T-junction • UV crosslinked (365 nm)	PEG	• PEGDA700 42.8% v/v, Irgacure 2959 6%, nanocrystals 5% • Oil: light mineral oil with 2% AbilEM90 and 0.05% Span-80	• None	[40]
	Up-converting nanoparticles	• Stop-flow projection lithography • UV crosslinked (365 nm)	PEG	• Code: PEGDA700 45% v/v, nanoparticles solution (0.5 mg/μl) 40% v/v, poly(styrenesulphonate) 10% v/v, Darocur1173 5% v/v • Probe: PEGDA700 18% v/v, PEG200 36% v/v, Darocur1173 4.5% v/v, aqueous buffer with probe 41.5% v/v	• Acrylated oligonucleotide (covalent) • During synthesis	[81]
	Quantum dots (QD)	• Droplet synthesis: flow-focusing, double T-junction, fusion chamber	Alginate	• 4% (w/w) and aqueous OPA:QDs in a 1:1 ratio (octylamine-modified polyacrylic acid-capped CdSe/ZnS QDs (OPA-QDs))	• IgG antibody (non-specific adsorption) • Post-synthesis	[53,65]

Table 1 (*continued*)

Encoding strategies	Synthesis technique	Hydrogel material	Pre-polymer composition[a]	Biomolecule immobilization if reported	Refs.
Quantum dots	• Chemically crosslinked • Droplet synthesis: T-junction with PTFE tubing • UV crosslinked (365 nm)	PEG	• Crosslinker: barium acetate (50 mM) • Oil: Soybean • PEG (PEGDA700, Darocur-1173, with silica colloidal particles) • Oil: oly (1,1,1-trifluoropropylmethylsiloxane) (x-22-821)	• Oligonucleotides (covalent) • Post-synthesis	[107,110]
Structural color (colloid nanocrystals)	• Droplet synthesis: capillary device with co-flows and flow-focusing • UV crosslinked (365 nm)	PEG	• PEGDA700 with SDS and Pluronic F-108 • Inner oil phase: ETPTA with QDs and silica nanoparticles to prevent QD aggregation; outer phase: hexadecane with AbilEM90	• None	[110]

[a] UV-sensitive photoinitiators are typically hydroxyalkylphenones: (HMOPP or Darocur1173 (= 2-hydroxy-2-methylpropiophenone), DMAP (= 2-dimethoxy-2-phenylacetophenone), Irgacure2959 (= 2-hydroxy-4′-(2-hydroxyethoxy)-2-methylpropiophenone). Irgacure is more water soluble than Darocur but requires longer exposure times.

structural integrity of the gel scaffold. Accordingly, the composition of the monomer blend and the polymerization conditions must be tuned to optimize the gel porosity, particle rigidity, and swelling behavior. Reaction kinetics and double bond conversion ultimately determine gel properties. Both are critically affected by the light intensity, the exposure time and the concentration of photoinitiator (typically 1–10% v/v) [42]. Increasing any of these parameters leads to greater double bond conversion, ultimately providing the gel with smaller pore size and higher structural rigidity. Detailed models of these parameters have been reported [42,43].

There is also value in altering PEGDA properties. Increasing the molecular weight of the PEGDA precursor and lowering its concentration in the prepolymer blend are effective ways to increase the gel porosity. Indeed, longer PEGDA chains or lower concentrations of active species result in a reduced crosslinking density. PEGDA precursors are typically diluted in aqueous buffers from 20% to 60% v/v (Table 1). It should be noticed though that at low PEGDA concentration, even at 20% v/v compositions, particles could display deformation and loss of mechanical stability under flow conditions [44].

Finally, the pore size can also be increased by adding an inactive porogen to the precursor solution, typically inert PEG [20,45]. The porogen, which is not covalently bound, can be washed away after gelation, leading to a higher porosity. Beebe and coworkers observed than the pore size enhancement using porogens was particularly effective for short PEGDA species (molecular weight <1000 g/mol) [20]. Indeed, adding PEG35,000 as a porogen to PEGDA700 led to macroporous gels, whereas the effects were minimal for PEGDA8000. The appearance of macropores results from polymerization-induced phase separation reaction [46]. Although the mixture of water and PEG species is initially homogenous, as the polymer chain grows, its solubility in water decreases, generating a polymer-rich phase and water-rich phase. Phase separation competes with the polymerization reaction and results in heterogeneous hydrogels with macropores.

2.1.1.3. Hybrid particles. Hybrid particles can be prepared by copolymerizing PEGDA with a second species, such as polylactic acid [47], chitosan [48,49] or polyacrylamide [50]. Hybrid particles can also contain varying concentrations of PEGDA along the length of the particle to give the particle greater structural rigidity [35,51]. Incorporating a second material can be a way to adjust the gel mechanical and chemical properties. For example, Jung et al. reported the synthesis of hydrogel particles functionalized with single-stranded DNA using a hybrid chitosan-PEG material [48,49]. The authors suggested a covalent binding mechanism between chitosan and PEGDA. Chitosan brings primary amines with low pK_a value ($\sim$6.5) into the material, which can be further engaged for conjugation of biomolecules with high surface density (Fig. 2a) [52]. However, pure chitosan is poorly soluble in organic solvents and aqueous buffers and yields hydrogels with low mechanical strength. Associating chitosan with PEDGA brings ease of fabrication and robustness.

Table 2
Reported bioassays.

Assay type	Target	Material	Probe (captured on gel particle)	Detection	Assay performance and multiplexing	Code	Comments	Refs.
Nucleic acid detection								
Hybridization assay	18nt oligonucleotide	PEGDA	Oligonucleotide (covalent)	Direct detection (FITC-labeled targets)	• Specific detection of SNP (3-plex) • No LOD	Shape		[33]
Hybridization assay	18–2nt oligonucleotide	PEGDA	Oligonucleotide (covalent)	Direct detection (FITC-labeled targets)	• Specific (3-plex) • LOD ∼single nM	Shape		[37]
Hybridization assay	21nt oligonucleotide	PEGDA + polyacrylamide	Oligonucleotide (covalent)	Complementary DNA	• Sensitivity: 0.66 pM	Structural color	• Comparison to glass beads and glass chip	[107,108,111]
Hybridization assay	20–200 nt oligonucleotides, microRNAs	PEGDA	Oligonucleotide (covalent)	Direct detection (PicoGreen or Cy3-labeled targets) or labeling with SAPE (biotinylated targets)	• 20–200nt targets: sub-attomole sensitivity • miRNA: 1 amol sensitivity	Graphical (extruded barcode)	• Mock complex environment using *E. coli* total RNA	[35,69]
Hybridization assay	15nt oligonucleotide	PEGDA	Oligonucleotide (covalent)	Direct detection (Cy3-labeled targets)	• Specific (2-plex) • No LOD	Color and graphical (bitcode)	• Particle mixing and immobilization using magnetic field	[38]
miRNA	microRNA	PEGDA	Oligonucleotide (covalent)	Universal labeling scheme with T4 DNA ligase; rolling circle amplification; fluorescence readout	• Single amol sensitivity and high specific in a 12-plex assay • Up to 300 aM sensitivity for 6 miRNA targets using amplification	Graphical (extruded barcode)	• High-through-put scanner • Detection from total RNA • 12-plex assay	[70,92]
mRNA	*in vitro* transcribed mRNA	PEGDA	Oligonucleotide (covalent)	Scheme using capture extender, label extender, fluorescence readout	• Specific (3-plex) • 6 amol sensitivity	Graphical (extruded barcode)	• Gel porosity tuned to accommodate diffusion of large mRNA	[45]
Protein detection								
Sandwich immunoassay	3 cytokines (IL-2, IL-4, TNFα)	PEGDA	Monoclonal antibodies (covalent)	Biotinylated secondary antibody + SAPE	• Specific (3-plex) • LOD (3σ): 1–8 pg/ml; dynamic range: 3 decades; CV: 8–11%	Graphical (extruded barcode)		[72]
Direct immunoassay	Human IgG	Alginate	Anti-human IgG (non-covalent)	Direct detection FITC-labeled target	• LOD (3σ): 2.2 μg/ml; dynamic range: 5–40 μg/ml	Spectral (QD)	• Code partially interferes with readout	[65]
Direct immunoassay	Rabbit anti-mouse IgG; anti-mouse IgM	PEGDA	IgG and IgM (covalent)	Direct detection FITC-labeled target	• Quantitative up to 500 ng/ml • Specific (2-plex)	Shape		[74]
Aptamer-based sandwich assay	α-Thrombin;	PEGDA	Aptamer sequence (covalent)	Biotinylated secondary aptamer or antibody + SAPE	• LOD: 21.7 pM (aptamer reporter); 4.09 pM (antibody reporter); CV: <10%	Graphical (extruded barcode)		[71]
Aptamer-based displacement assay	Adenosine, thrombin, IgE	PEGDA	Complementary oligonucleotide to aptamer sequence (covalent)	Target induces the release of the fluorescently labeled aptamer probe from particle	• Specific detection of 2 mM targets (3-plex)	Structural color and shape		[50]

Table 2 (*continued*)

Assay type	Target	Material	Probe (captured on gel particle)	Detection	Assay performance and multiplexing	Code	Comments	Refs.
Small molecule detection								
Enzymatic assay	Glucose	PEGDA	GOX/HRP (encapsulation)	Conversion of Amplex®Red into a fluorescent product	• LOD: 0.2 mM	Shape		[67]
Enzymatic assay	Glucose	Alginate	GOx (encapsulation)	Conversion of Amplex®Red into a fluorescent product	• Quantitative	none (monoplex)		[109]
Enzymatic assay	Glucose	PEGDA	TRITC-ConA/ FITC-Dextran (encapsulation)	FRET assay	• Dynamic range: 1–10 mM	None (monoplex)		[39]

Abbreviations: CV: coefficient of variation; FITC: fluorescein isothiocyanate; GOx: glucose oxidase; FRET: Förster resonance energy transfer; HRP: horseradish peroxidase; LOD: limit of detection; QD: quantum dot; SAPE: streptavidin phycoerythrin; SNP: single nucleotide polymorphism; TRITC-ConA: tetramethyl rhodamine isothiocyanate concanavalin A.
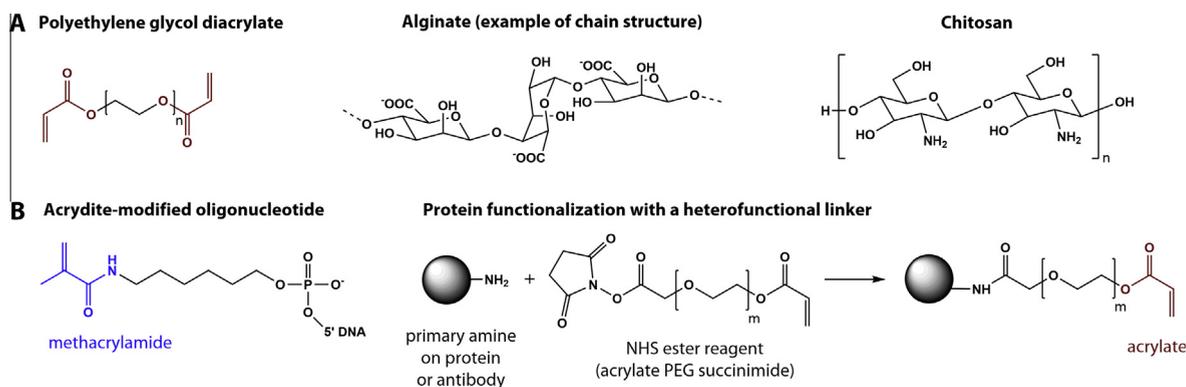
Fig. 2. Examples of commonly used chemistries to construct hydrogel particles. (A) PEG-DA subunit, alginate subunit and chitosan (which has been blended into PEG particles). (B) Examples of biomolecule functionalization to enable covalent incorporation into hydrogel meshes including acrydite modified DNA and attaching acrylated linkers using amine chemistry on proteins.

2.1.2. Alginate

Recent publications report the fabrication of encoded particles made of alginate gels and their potential sensing applications [53–55]. Alginate is a naturally available anionic polysaccharide that is extracted from brown algae and can be precipitated into alginic acid at low pH (1.5–3.5). Sodium alginate is commercially available in a wide range of molecular weights from 32,000 to 400,000 g/mol [56].

Alginate can be crosslinked in the presence of multivalent cations, typically calcium (Ca^{2+}) and barium (Ba^{2+}) divalent ions. Its structure has been shown to be a mixture of unbranched copolymers containing different sequences of (1,4)-linked-ß-D-mannuronate (M) and α-L-guluronate (G) residues (Fig. 2a) [57]. The interaction between the cations and the carboxylic groups of the polysaccharide induces gelation, and it is now believed that only G-blocks are involved in intermolecular cross-linking [56]. The hydrogel physical properties, such as its porosity and stiffness, depend on alginate composition (molecular weight distribution, G block/M block ratio and sequence) and on the stoichiometry of the alginate with the divalent cation.

Due to its biocompatibility and requirement for mild gelation conditions, alginate is an attractive and cost-effective material for biomedical applications. Thus, alginate and modified alginate hydrogels [58] have been investigated for tissue engineering [59], drug delivery [60,61], cell encapsulation [62,63] and wound healing [64] applications. Regarding sensing applications, alginate solution droplets (1–5% w/w) were crosslinked with either barium acetate [53] or calcium chloride solutions [54,55] to form quantum dot-doped particles [53], multi-compartmental particles with fluorescent nanobeads [54] and particles encapsulating sensing liposomes [55].

2.2. Immobilizing bioprobes on hydrogel particles

Defining a reliable strategy for the immobilization of bioreceptors within the support material is a critical step for the fabrication of a biosensing array. Major criteria to take into account are: the availability of reactive groups on the substrate and biomolecule (or possibilities to modify as needed), the type of immobilization (covalent, non-covalent), and the risk for biomolecule degradation in the coupling conditions (UV exposure, free radicals, temperature, organic solvents).

2.2.1. Physical adsorption and encapsulation

Ji et al. investigated the possibility to immobilize unmodified antibodies on optically encoded crosslinked alginate particles through physical adsorption [65]. Physical adsorption does not require reactive chemical groups and typically proceeds through a simple incubation step. Although the resulting particles were then successfully engaged in a proof-of-concept immunoassay, physical adsorption techniques often result in bioreceptor leaching or high non-specific adsorption.

While this first example involved a post-synthesis modification of the particle, another strategy consists in physically entrapping the bioprobe in the hydrogel mesh at the time of gelation. Indeed, voluminous sensing entities present in the monomer solution may remain captured inside the gel upon crosslinking, if the pore size is small enough. Accordingly, enzymes (horseradish peroxidase (HRP), glucose oxidase (GOx) [66,67] and concanavalin A [39]) have been encapsulated within PEGDA575 or PEGDA700 particles for glucose sensing applications. Such protocols require tightly crosslinked gels to prevent probe from leaching out, especially in high swelling saline conditions. This limits the ability to freely tune pore size of the gel and prevents access for large targets (further discussed in Section 2.3). In these examples, the target (glucose) and detection molecules (hydrogen peroxide, Ampliflu™Red) were small enough to diffuse efficiently through the tight gel mesh (pores ~1 nm).

In another study, Park et al. showed that increasing the molecular weight of the PEGDA precursor from 575 to 3400 g/mol resulted in improved kinetics for glucose read-out at the cost of higher probe leaching, due to an increased porosity [36]. To circumvent the leaching issue, the authors covalently captured the enzyme on magnetic nanoparticles of larger diameter (~30 nm) first, that were then efficiently embedded within the hydrogel mesh. It is worth noticing that encapsulation methods can be used

not only for the probe immobilization but also for loading the particle with entities that will confer additional properties to the gel such as magnetic properties (super-paramagnetic particles [68]) or spectral encoding (quantum dots [65]).

2.2.2. Covalent immobilization in PEGDA gels during particle synthesis

Copolymerizing the bioprobe with the gel material, when possible, guarantees a stable immobilization and overcomes leaching issues. The probe is functionalized with a polymerizable moiety beforehand and added to the monomer solution before polymerization. Acrylate and methacrylate modifications have been widely explored to covalently anchor biomolecules in PEGDA during the free-radical polymerization reaction (Table 1).

2.2.2.1. Oligonucleotides. The Acrydite™ phosphoramidite modification introduces a UV-polymerizable methacrylamide group on an oligonucleotide probe (Fig. 2b). Most reports of PEGDA sensing particles rely on the Acrydite™ group chemistry [33,35,37,38,45,69–71]. Meiring et al. compared oligonucleotide immobilization in PEGDA575 particles in the presence or absence of a 5′-methacrylamide modification [33]. The 18-mer bioprobes were fluorescently labeled to assess incorporation yields. The fluorescence appeared dramatically increased in the case of the covalent immobilization, demonstrating the efficiency of covalent binding over physical entrapment. Moreover, when soaking particles in deionized water for 24 h, over 95% of the covalently bound oligoprobes remained captured.

Similarly, Pregibon et al. copolymerized 5′Acrydite™-oligonucleotides (50-bp) with PEGDA700 solutions ranging from 15% to 35% v/v (PEG200 was used as porogen) [35]. The authors observed a linear probe incorporation, ranging from ~5% to 25%. According to the authors, this trend can be explained by the linear propagation rate with respect to double-bond concentration observed for multifunctional, reactive monomers. The authors suggested that efforts in matching the reaction rates of the monomer and probe species could possibly increase incorporation efficiency, as acrylates are known to react faster than methacrylates.

2.2.2.2. Proteins. A similar approach was used to immobilize proteins and antibodies into PEGDA particles. The Doyle group reported the functionalization of antibody probes using a 2 kDa heterobifunctional PEG linker [72]. An acrylate moiety on one end guaranteed copolymerization with the gel, whereas and an N-hydroxysuccinimide (NHS) activated ester on the other end captured primary amines on the protein side chains (Fig. 2b). Probe antibodies were incubated with the linker at room temperature and the resulting mixture was directly added into the monomer blend before polymerization. Notably, although others have reported the precipitation of unmodified proteins in PEG monomer mixes, no solubility issues were observed after PEGylation [18].

The incorporation of antibodies in the hydrogel was higher than for oligonucleotides for similar monomer compositions (respectively 26% and 10%). Although the

immobilization mechanism was not elucidated, the authors suggested two causes for this increased efficiency: the presence of multiple PEGylation sites on the protein and the possible direct photopolymerization reaction of thiol groups on amino acids side chains [73]. The immobilized antibodies efficiently captured their antigen in spite of the exposure to UV radiations and free radicals. Other commercially available heterobifunctional linkers target cysteine residues on proteins in order to incorporate an acrylate moiety on the protein.

2.2.3. Post-synthesis covalent immobilization

Finally, an alternate strategy consists in covalently immobilizing biomolecules in the particles after the gelation. For PEGDA gels, however, such an approach requires adding functional groups beforehand to the gel monomer structure. Park et al. incorporated carboxylic acid groups in PEGDA particles using a copolymerization reaction with acrylic acid [74]. Those groups were then converted into reactive esters moieties to capture proteins through 1-ethyl-3-(3-dimethylaminopropyl)-carbodiimide/N-hydroxysulfo-succinimide chemistry. The lack of specificity of functional group though makes it difficult to functionalize several types of particles simultaneously.

Work by the Herr group has indicated the possibility to also couple biological species into gels using biotin–streptavidin interactions [75]. Likewise, Jung and Yi copolymerized PEGDA with chitosan, resulting in particles with reactive primary amines with low pK_a value (~6.5) [48,49]. A heterobifunctional linker captured those amino groups on one end while reacting with an oligonucleotide or protein through a copper free click-chemistry reaction on the other end. The authors applied this strategy to functionalize particles with oligonucleotides used as anchors to assemble supramolecules (tobacco mosaic virus) with high density on the particles [48]. The virus further served as a template to conjugate multiple proteins on the gel surface [76].

2.3. Hydrogels in biosensing applications

The three-dimensional nature of hydrogels may affect the sensitivity of biosensing assay. Those considerations must be taken into account when selecting a material for a particle-based assay.

2.3.1. Particle swelling

Salt-containing solutions typically cause hydrophilic gels to swell and to uptake more water, but these behaviors can vary based on the composition and charge of the gel. Since hydrogel microparticles should be able to robustly detect analytes in biological samples, it is important to understand their swelling behavior in aqueous solutions that could contain physiologically-relevant (~140 mM) or high (200–400 mM) salt concentrations that are necessary for nucleic acid binding. A thorough characterization of these behaviors would allow researchers to ensure that gel swelling does not affect concentration of entities that are physically immobilized within, assay conditions or particle decoding (for example due to anisotropic swelling that could deform a graphically encoded particle).
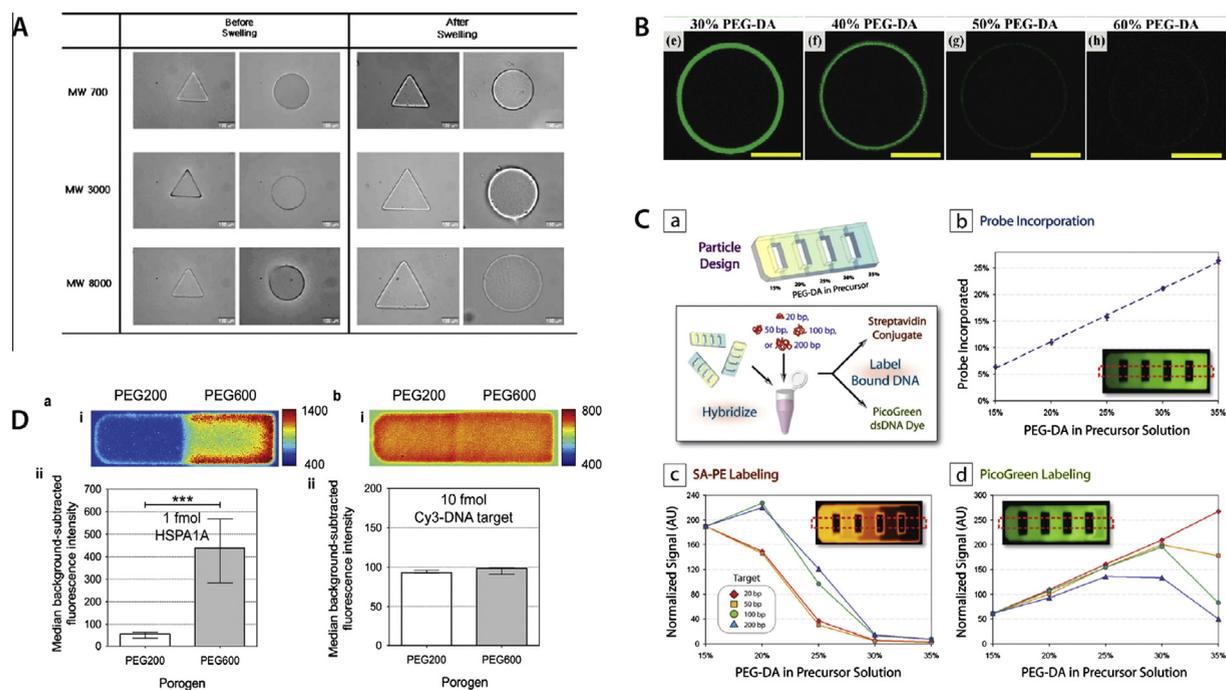
Fig. 3. Characterization of hydrogel particles. (A) PEGDA particle swelling changes depending on starting molecular weight of PEG chains. Reproduced from [67]. Copyright 2008 Springer. (B) Confocal z-scan images reveal that DNA target hybridization profiles depend on crosslinking density of particles Reproduced from [37]. Copyright 2010 ACS. (C) Systematic characterization of encoded gel particles show that increasing PEG-DA in precursor solution leads to greater functionalization efficiency but limits penetration of larger DNA molecules. Penetration ability also depends on size of labeling analyte. Reproduced from [35]. Copyright 2009 ACS. (D) Comparison of porogens in fabrication of gel particle arrays shows that PEG600 leads to the larger pore size required for mRNA detection in comparison to use of PEG200. Use of smaller targets confirms that functionalization efficiency of probe is not compromised by using PEG600 as a porogen. Reproduced from [45]. Copyright 2012 ACS.

The theory behind swelling behavior of crosslinked hydrogels in different chemical environments has been extensively discussed in previous reviews [4,5]. Few groups also empirically examined swelling of gel particles made from different starting compositions. One study focused on the effect of the molecular weight of the PEGDA precursor on the swelling of shape-encoded particles (Fig. 3a). The amount of swelling increased with the precursor molecular weight (40% for PEGDA700, 80% for PEGDA3400). However, the particle deformation was isotropic and the overall shape and aspect ratio were not affected [36,67]. Another study found that increasing the percentage of PEGDA in the prepolymer solution increased the tendency of particles to uptake water immediately after polymerization [33].

2.3.2. Probe density

Due to their three-dimensional nature and increased effective surface area, hydrogel substrates offer higher capacity for bioprobe immobilization in comparison to surface-based systems such as planar microarrays or polystyrene beads. Similar starting concentrations of the probe solution generate greater effective projected densities on the gel (projection the 3-D gel onto 2-D) than on a surface since there is functionalization throughout the gel [26,71]. Assuming first-order Langmuir kinetics for the target/probe interaction, this increased density leads to more

target/probe complexes formed at equilibrium and hence a better assay sensitivity [71]. Srinivas et al. reported an effective oligoprobe density of 10^5 molecules per μm^2 on PEGDA gel particles prepared from a 10 μM probe solution. This probe concentration is at least one order of magnitude denser than on an equivalent microspot [71].

Zubtsov et al. carried an extensive comparison between surface spots and gel pads for antibody immobilization [26]. On surface spots, the relatively large molecular size of antibodies limited the effective density to 10^4 molecules per μm^2. Increasing the probe concentration in the spotting solution did not necessarily lead to greater probe density. Furthermore, at maximum capacity, molecules were separated only from ∼10 nm, which may restrict the target accessibility to those probes. Hydrogel substrates overcome those constrains: optimized immobilization conditions on gel pads provided up to 10^7 molecules μm^{-2} and an approximate 100 nm separation between molecules. Notably, however, miscibility of probe molecules into the more hydrophobic monomer solutions could pose an upper constraint on maximum achievable homogenous probe concentration throughout the gel [72].

2.3.3. Probe accessibility and target diffusion

The second critical factor for assay sensitivity is the ability of target to diffuse freely throughout the volume of the gel and to access inner probe molecules. Indeed, if

the mesh is too tight, large biological targets might not be able to penetrate the network or enter only at very low diffusion rates, significantly delaying approach to equilibrium. Meanwhile, if the gel is too porous, functionalization efficiency of probe molecules could be significantly lower than optimal, which would also affect sensitivity [35]. The porosity of hydrogel microparticles can be adjusted to allow diffusion and reaction of biological entities of different size including proteins, microRNA, and antibodies and mRNA (respective typical radii of gyration r_g: 2 nm, 3 nm, 6 nm and 10 nm) [45].

2.3.3.1. Hydrogel pads. Target diffusion and probe/target interaction kinetics in hydrogel substrates were first extensively studied and modeled for hydrogel pads [25,26,77] and hydrogel posts [20]. Sorokin et al. compared the kinetics of oligonucleotide hybridization on gel pads with surface microspots [25]. Although the gel array showed slower hybridization kinetics due to hindered diffusion of analytes within the porous gel mesh, the fluorescence signals when the assay came to thermodynamic equilibrium were stronger. The increase in signal was attributed both to better thermodynamic association constants of binding and to the higher effective probe density in the gel environment.

Indeed, it has been previously demonstrated that solution-phase hybridization poses the lowest energy barriers for nucleic acid binding. Solid-phase hybridization suffers from higher free energies of binding because targets need to diffuse through densely packed probe regions, creating steric constraints [78]. The gel environment appears closer to the ideal solution limit due to the high water content and to the sufficient space between probe molecules despite a higher effective probe density. Accordingly, observed free energies of binding were actually lower for nucleic acid binding relative to a standard microarray. The reduction of steric hindrance provides not only better sensitivity, but also better specificity, since there is less tolerance for mismatch sequences when probe molecules are spaced further apart [25].

Zubstov et al. performed similar studies for protein-based gel chips [26]. Once again, the gel environment enhanced protein detection. The signal enhancement, however, was primarily due to the increased probe immobilization efficiency inside the gel with no significant difference between kinetic rates of signal saturation for surface spots and gel pads.

2.3.3.2. Hydrogel particles. Similarly, target binding inside hydrogel particles has been investigated through experiments as well as modeling. Using both approaches, Pregibon and Doyle characterized diffusion and reaction inside a well-mixed gel particle array [35]. In particular, the authors considered the rate of target-probe association to the rate of analyte diffusion into the gel particles, defined as the Dahmköhler number (Da). The study showed that the gel array was mass-transport limited since reaction occurred significantly faster than diffusion throughout the gel (Da ≫ 1). These characteristics can lead to restricted target penetration depth, confining the majority of signal at the outer edge of the gel particles at low target concentrations. That confinement has been observed in a number of studies (Fig. 3b) [37,38,69,74].

The gel composition should be finely tuned to optimize target diffusivity and hence assay sensitivity. An extensive optimization of the composition of PEGDA700 hydrogel particles for the quantitative detection of oligonucleotide targets of increasing length (20, 50, 100 and 200 bp) demonstrated that Increasing PEGDA concentrations caused reduced diffusion of the largest targets (Fig. 3c) [35]. Such diffusion considerations should not be limited to targets but should be applied to any molecule required for signal generation. Indeed, bulky labels such as streptavidin–phycoerythrin might also face restrictive diffusion constraints (Fig. 3c) [35].

As mentioned earlier in this section, increasing the molecular weight of the PEGDA precursor and/or adding a porogen species are additional ways to enhance the porosity of PEGDA particles and improve target diffusivity. For example, Choi et al. successfully adapted a particle-based assay designed for small miRNA targets ($r_g \sim 3$ nm) to full-length mRNA targets ($r_g \sim 10$ nm) by replacing the PEG200 porogen with PEG600 (Fig. 3d) [45]. The authors showed clear evidence of the significant steric hindrance arising with the smaller porogen by using hydrogel posts as model systems to study solute diffusion.

In conclusion, the gel should be designed to mitigate effects arising from swelling behavior, be porous enough to allow target diffusivity, but still be dense enough to preserve a large reactive surface area with high probe densities. Particles should also retain their mechanical integrity and structural stability through the course of the assay. For optimal hydrogel composition, each probe/target pair and assay conditions should be taken into consideration in order to balance these phenomena.

3. Synthesizing encoded hydrogel particles

We discussed the chemical nature of the hydrogels commonly used for particle-based bioassays, as well as the gel crosslinking and probe immobilization reactions at the molecular level. We will now review techniques for fabricating particles of controlled morphology and size. In most examples considered throughout this review, particle dimensions fall in the micron range (10–1000 μm).

Conventional methods for the fabrication of micrometer-sized hydrogel particles include dispersion, precipitation, and emulsion polymerization techniques [79]. However, these approaches are often limited to the production of spherical particles with uniform surface properties and cannot achieve monodispersity. Furthermore, these techniques may require organic solvents and high temperature conditions, which are typically incompatible with biomolecule stability. Nevertheless, recent advances in microfabrication techniques [11–14,80] have opened new avenues to produce complex particles, in mild chemical conditions and with high reproducibility and monodispersity. New routes to chemically and structurally anisotropic hydrogel particles have considerably expanded strategies for hydrogel particle encoding.

3.1. Building a library of encoded particles

Multiplexed assays using suspension arrays require techniques for individual particle encoding. Indeed, as particles are pooled and mixed in the sample for target capture, a unique particle code is essential to identify each particle and corresponding probe-target couple at the time of assay readout. The code must also remain unaffected by the assay conditions, and its readout must be orthogonal to the signal of target reporters and optical labels involved in the assay to prevent convolution. Numerous encoding strategies and substrates (including spherical latex, silica, or glass particles, as well as metallic nanowires) have been investigated over the years for bead-based arrays and have been thoroughly reviewed by others [29,82,83]. The vast majority of reports are based on spectrally-encoded beads involving fluorophores, quantum dots, photonic beads or photo-bleached microspheres [29]. Suspension arrays of polystyrene particles with up to 500 unique fluorescence signatures are now commercially available for nucleic acid tests and immunoassays [84,85]. However, spectral overlap limits the size of the code library. In contrast, more recent approaches have focused on the fabrication of anisotropic particles with tunable non-spherical shapes and internal features, allowing graphical encoding [83].

Hydrogel particles have been encoded using both spectral and graphical codes (Fig. 4). Table 1 presents the various encoding strategies reported in the literature along with particle fabrication techniques. In all cases, the particle synthesis technique and the encoding strategy are tightly linked. One class of synthesis platforms utilizes photolithographic techniques for generation of particles with pre-defined geometrical patterns from UV-curable monomer. Additionally, the recent advances in droplet generation techniques, especially droplet microfluidics, have led to innovative production methods of spherical hydrogel particles that can be optically encoded. Particle encoding generally occurs at the time of synthesis.

3.2. Photolithographic methods for graphical encoding

Most hydrogel particle arrays reported in the literature were generated from the UV-induced polymerization of PEGDA. Top-down particle fabrication techniques take advantage of this photopolymerization step to pattern particles in two dimensions. Specific shapes or internal features, such as extruded holes, can be generated to create graphical codes. The shapes and/or internal features imposed on the particle are typically fabricated using one of two strategies: by using a photomask to limit UV illumination to specific regions, or by particle molding on a polymeric mold with negative features. Fig. 5 presents the corresponding workflows.

3.2.1. Contact photolithography
3.2.1.1. Patterning shapes. In 2004, Meiring et al. reported the first example of graphically encoded hydrogel particle array for biosensing, named MUFFINS for *mesoscale unaddressed functionalized features indexed by shape* [33]. The authors adapted photolithographic fabrication techniques

originally developed for the production of submicron features in the semiconductor industry [12], to the production of millimeter-sized PEGDA particles functionalized with oligonucleotides. A blend of PEGDA monomer and acrylated oligonucleotides were poured onto a Teflon substrate and covered with a photomask placed in direct contact with the pre-polymer. The mask consisted of a laser-printed transparency film mounted on a glass slide. Most of the mask was black with transparent features for reproduction of particles with desired shape and size. When the device was exposed to UV light through the photomask (approximately 200 mJ cm^{-2}, broadband UV), the light was blocked by dark areas and could only reach regions of the material beneath the transparent portions of the mask. Only these illuminated regions crosslinked into particles, transferring the shape pattern to the hydrogel (Fig. 5a). Finally, the uncrosslinked pre-polymer was washed away and the patterned hydrogel particles were physically detached from the mask on which they adhered. As a result, the authors successfully synthesized 1 mm hydrogel particles shaped as squares, triangles, circles, and crosses. All these encoded particles were functionalized with different methacrylated oligonucleotides during the free radical polymerization (Fig. 4a).

3.2.1.2. PDMS devices. Later studies reported the use of polydimethylsiloxane (PDMS)-based devices for producing shape-encoded particles through static contact photolithography. Conveniently, PDMS prevents particle adhesion to the substrate, enabling easy collection of the formed particles. Indeed, oxygen can diffuse through PDMS and locally inhibit the polymerization reaction on the surface substrate [43]. PDMS devices were used to produce 200 μm long PEGDA particles that were shape-encoded and functionalized with antibodies for immunoassays [74] or with enzymes (GOx, HRP) for glucose sensing [36,67,86] (Fig. 4b).

One synthetic approach consisted of simply sandwiching the pre-polymer solution between PDMS-coated glass slides [36,74]. In a second approach, the monomer was enclosed in a rectangular 50 μl PDMS chamber (2 cm × 4 cm × 50 μm) sealed with a PDMS-coated glass slide [67]. Using a chrome soda lime photomask with a 40 × 80 array of features, the authors polymerized ∼3000 hydrogel microparticles per UV exposure (1 s, 365 nm, 300 mW/cm^2). Well-resolved particles with sizes ranging from 50 μm to 200 μm were obtained, although a significant difference in particle diameter between the mask and the polymerized feature was observed for the smallest particle size (20%).

3.2.1.3. Dual encoding through shape and color. Notably, Ye et al. reported the fabrication of an array of particles indexed by both shape and structural color, for aptamer-based detection of proteins [50]. In addition to a unique geometrical shape, the photonic crystal hydrogel microsensors displayed unique brilliant colors and particle reflection spectra originating from light diffraction inside the particle (Fig. 4c). With a negligible fluorescence background, such particles are compatible with fluorescence-based assays.
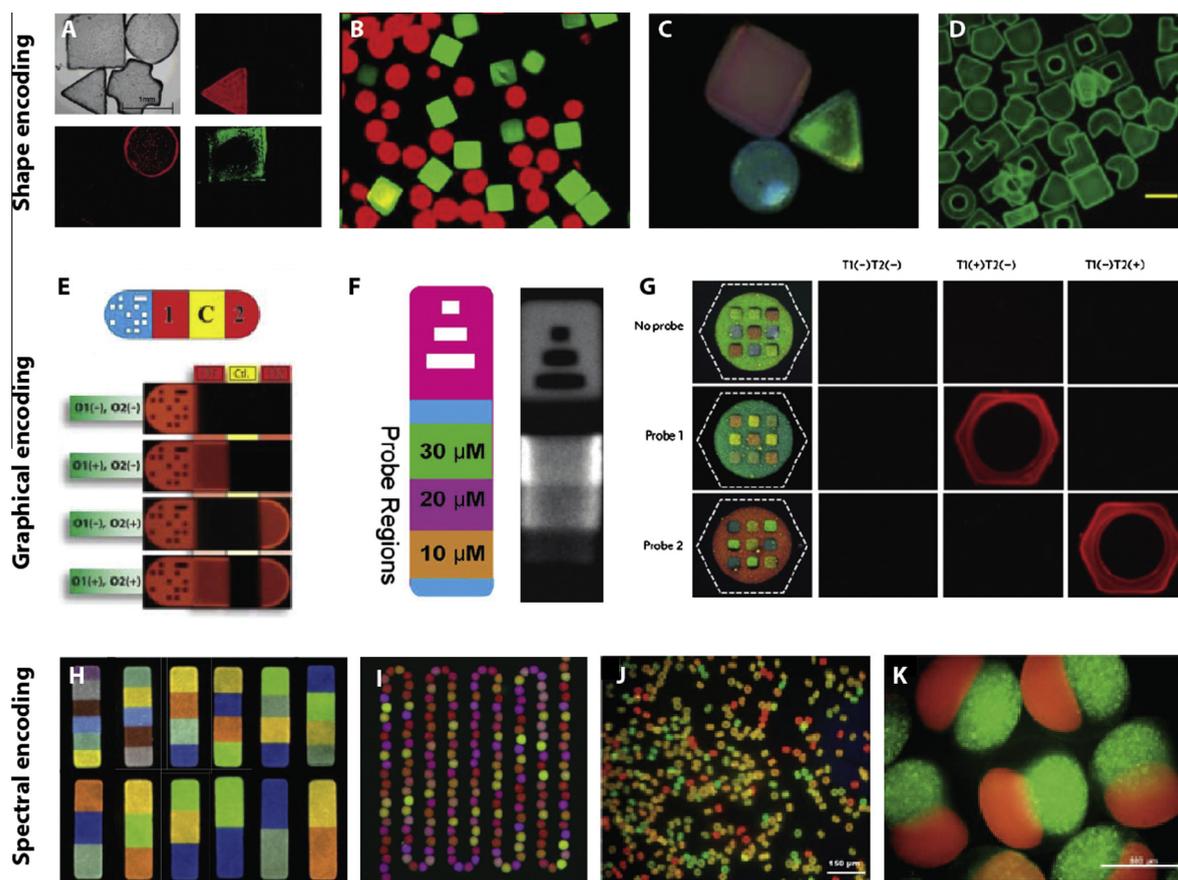
Fig. 4. Overview of strategies for particle encoding. **Shape encoding**: Particles polymerized using contact lithography (A) for DNA assay. Reproduced from [33]. Copyright 2004 American Chemical Society and (B) for enzyme assay. Reproduced from [67]. Copyright 2008 Springer. (C) Particles doped with photonic crystals. Reproduced from [50]. Copyright 2011 RSC. (D) Particles fabricated via replica molding. Reproduced from [37]. Copyright 2012 ACS. **Graphical encoding**: Particles polymerized using flow-lithography with (E) 2D-barcode. Reproduced from [69]. Copyright 2007 AAAS. (F) 1D-barcode. Reproduced from [71]. Copyright 2004 American Chemical Society and (G) color-barcode. Reproduced from [38]. Copyright 2010 NPG. **Spectral encoding**: (H) Optical barcodes using upconverting nanocrystals. Reproduced from [81]. Copyright 2014 NPG. (I) PEGDA spheres encapsulating downconverting nanocrystals. Reproduced from [40]. Copyright 2012 RSC. (J) Quantum-dot tagged alginate microparticles. Reproduced from [65]. Copyright 2011 RSC. (K) Janus alginate microparticles encapsulating liposomes. Reproduced from [55]. Copyright 2012 ACS. (For interpretation of the references to color in this figure legend, the reader is referred to the web version of this article.)

The particle fabrication process involved two polymerization steps. First, a PEGDA monomer blend was mixed with a suspension of monodisperse colloidal silica nanoparticles (150 nm) and used to polymerize shape-encoded particles (500–1000 μm; thickness 125 μm) between quartz slides using contact lithography. HF etching then degraded the silica nanoparticles, resulting in an inverse nanoporous structure imprinted in the gel that conferred the structural color to the particle. Then, an additional acrylamide-based layer polymerized on top of the PEGDA material enabled covalent capture of acryloyl-modified oligoprobes in the particle.

3.2.1.4. Key parameters for photolithography. The resolution of the imprinted features is a critical parameter for graphical encoding. Particle edges and overall shape should be sharp, well resolved, and highly reproducible among particles to ensure a reliable decoding process. In case of contact photolithography, the resolution mainly depends on

the light source collimation and photomask quality. Although a laser-printed transparency will provide sufficient resolution to prepare particles in the range of 100–1000 μm [87], finer resolution often demands more costly and time-intensive techniques, such as chromium-on-glass mask writing. The quality of UV illumination is an additional key parameter for the reproducibility and resolution of the imprinted features. Indeed, the UV light intensity should be even across the entire illumination area in order to generate reproducible particles. Proper collimation is critical to achieve a high resolution and the light intensity imposes the exposure time required for polymerization [42].

3.2.2. Flow lithography

The contact lithography techniques described above rely on static batch processes with limited throughputs. Particle collection time and set-up times in between runs reduce the synthesis rate. In 2006, the Doyle group
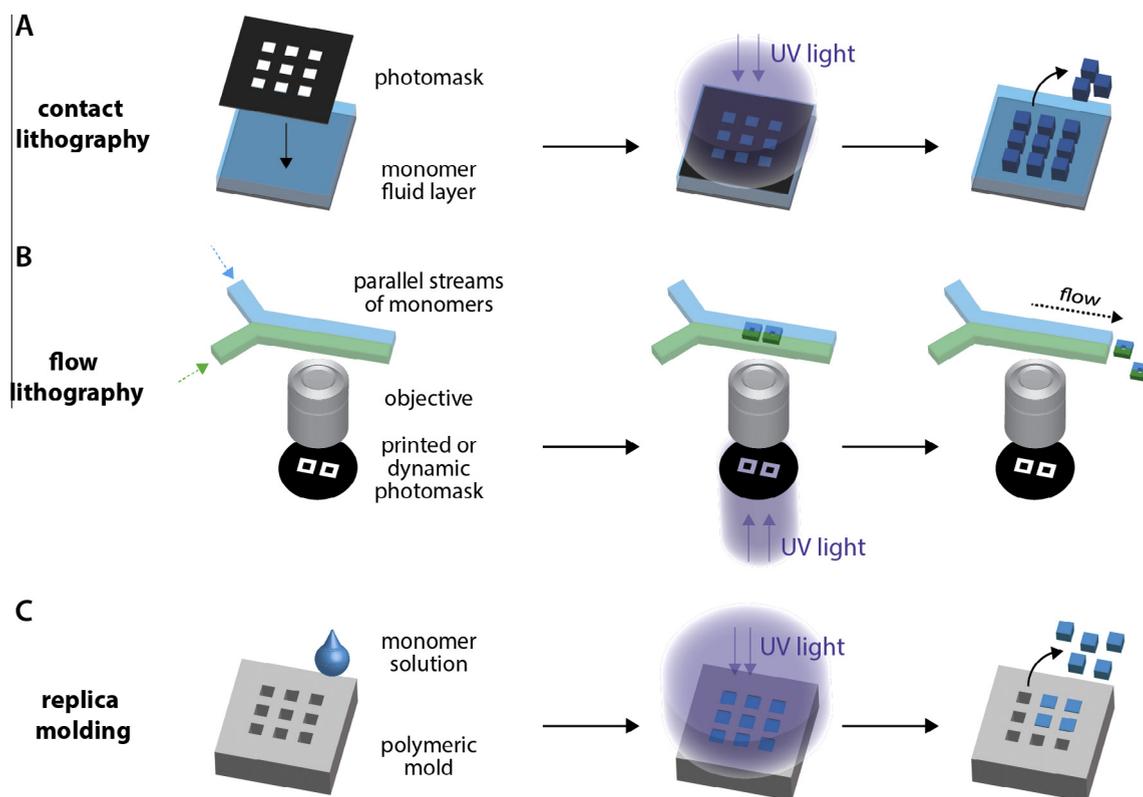
Fig. 5. Photolithography methods for particle synthesis. (A) Contact lithography: a photomask is placed in direct contact with monomer solution. (B) Flow lithography: photomask designs are projected onto streams inside microchannels. (C) Replica molding: features created using soft lithography are used to impart designs onto soft hydrogel particles.

reported an innovative method for the continuous production of hydrogel particle using flow-lithography [88–90]. Fabricating particles under flow in a PDMS microfluidic device enabled dramatic increase in production throughput (up to 18,000 particles per hour).

3.2.2.1. Stop-flow lithography. Fig. 5b presents a typical workflow for flow-lithography. The PDMS microfluidic channel is filled with PEGDA monomer using a pressure-driven flow. The device is then exposed to UV light through a photomask to induce particle formation inside the microfluidic channel. Oxygen permeation through PDMS creates local inhibition of the polymerization reaction near the channel walls, resulting in formation of free-floating particles [43]. Activating the flow pushes particles towards the channel outlet, where they can be collected. Subsequently, another synthesis cycle can take place in the channel filled with fresh monomer. The particle thickness is determined by the channel height (20–50 μm) and the thickness of the oxygen inhibition layer (typically ~2.5 μm) [43].

In contrast to previous approaches, the photomask is typically not placed in direct contact with the device. The microfluidic device is placed on the stage of an inverted microscope and the mask is placed in the field stop position, projecting the mask pattern onto the monomer layer through the objective. The great degree of control over

light focus leads to creation of uniform particles [89]. Upon projection through the microscope objective and internal lenses, the pattern size is reduced. This reduction enables further reduction of the minimum size of particles.

In comparison to contact lithography techniques, the restricted field of view limits the number of particles that can be synthesized per UV exposure. However, the UV light condensation through the objective leads to dramatically shortened exposure times (tens of milliseconds instead of seconds) and the overall cycle time is on the order of a second. Using projection flow-lithography, the authors reported particle throughputs as high as 18,000 particles per hour (~250 μm × 70 μm particles) and throughputs could be further increased [51].

3.2.2.2. Graphical barcodes. Complex graphical codes (extruded holes, shapes) can be patterned using projection flow lithography as long as codes are reliably polymerized. Accurate polymerization of well-resolved particles with sharp code regions required precision with respect to focal plane and alignment between the projected pattern and the narrow channel. Although the barcoding technique was originally developed to operate under continuous flow [88], stopping the flow during UV exposure (stop-flow lithography) was shown to improve particle resolution up to micrometer precision, light diffraction being the ultimate limit to the mask feature size [89]. In 2007,

Pregibon et al. fabricated an array of extruded particles using 2D dot-coded scheme possibly leading to millions of uniquely graphically encoded particles (Fig. 4e) [69]. Later, the group reported multiple applications of 1D-barcoded particles in multiplex bioassays (Fig. 4f) in the field of nucleic acid detection (oligonucleotide, miRNA, and mRNA [35,45,70]) as well as protein detection [51,71].

3.2.2.3. Chemically anisotropic particles. In addition, exploiting laminar flow properties in microfluidic devices enable to generate chemically anisotropic and graphically encoded particles in a single UV exposure. Indeed, under laminar flow conditions, multiple monomer solutions (introduced through different inlets) form a co-flow in the main channel and remain as parallel streams with negligible mixing. Upon UV exposure, the polymerized particle will therefore have spatially segregated regions bearing different chemical functionalities depending on the number of co-flowing streams in the device. The stream widths can be easily tuned by adjusting the relative pressure driving each flow [91].

In the first demonstration by Pregibon et al. in 2007, two streams were co-flowed in the same device [69]. One stream had PEGDA mixed with an acrylated rhodamine to provide a fluorescent barcoded region, and the other stream contained acrylated DNA probes used for sensing. The photomask used imparted the bit-code design to the fluorescent stream. Since the two regions of the resulting particle were spatially segregated, single-wavelength excitation could be used both for decoding the particle identity and for quantifying the target after hybridization and fluorescence labeling. The authors also demonstrated ability to synthesize multiple target capture regions on the same particle to use a single particle to measure several markers.

Further applications of SFL have led to creation of multifunctional particles bearing distinct intraplexed regions for different proteins [72], microRNAs [92], or with varying probe concentrations [71]. The latter can been exploited for assay development or to expand assay dynamic range or sensitivity [71]. Additionally, in a recent report, up to six chemistries were used to pattern spectral barcodes using up-converting nanoparticles [81] (Fig. 4h). Notably, recent iterations have extended the technique to non-oxygen permeable devices using hydrodynamic focusing and inert fluid streams enabling vertical layering [93,94]. Particles with significantly smaller heights (∼2–6 μm) were also fabricated using oxygen-controlled flow lithography [95]. Strategies to make 3-D particles using stop-flow lithography were also recently reported [96,97].

3.2.2.4. Color-coded particles and dynamic masking. Flow lithography was further developed by the Kwon group to use a digital micromirror device in place of a static mask [98]. A computer-controlled digital micromirror device (two-dimensional array of micro-mirrors) gives dynamic control over the projected UV exposure pattern, enabling real-time modification of the microstructures to pattern. Moreover, the large field of view increases the number of particles that can be polymerized per exposure.

This technique was applied to the synthesis of multifunctional particles for multiplex DNA detection with complex codes [38]. The graphical encoding used a combination of a binary barcode (bit sequence) and spectral code, as the bits displayed eight different colors (Fig. 4g). With a 10-bit sequence, 8^{10} unique codes could potentially be generated. To polymerize color-coded bits, the authors used a PEGDA pre-polymer solution containing superparamagnetic colloidal nanocrystal clusters, named *M-ink*. The modulation of an external magnetic field induced the reorganization of the nanocrystal clusters structure, resulting in a color shift of the ink solution. The spatially controlled UV exposure triggered the gel crosslinking at desired bit position, thereby fixing its color. The color and position of the next bits were simply adjusted by tuning the magnetic field intensity and changing the dynamic projected light pattern. The production of barcoded particles with eight different colors was achieved in approximately 1 s, with a unique ink solution. The technique however required a second solution and an alignment step for polymerizing a target capture region that was spatially separated the code region.

3.2.3. Replica molding

Instead of using a photomask to create a patterned UV illumination, it is possible to use a polymeric substrate patterned with negative features to mold shape-encoded particles. Fig. 5c presents the usual workflow for replica molding (also known as imprint lithography), which is directly inspired from the soft lithography techniques developed for the fabrication of microfluidic devices [12]. Typically, a liquid UV-curable monomer (usually PEGDA) is poured into an array of shape-encoded wells. After removal of excess material if necessary, UV light exposure induces gel crosslinking and form individual particles in wells.

The DeSimone group first reported the fabrication of sub-200 nm to micron scale hydrogel particles via replica molding in 2005 [99]. For the "PRINT" method (*Particle Replication In Nonwetting Templates*), the authors used a non-wetting perfluoropolyether (PFPE) as the mold material to confine the liquid monomer into the isolated cavities. Applying the material onto the mold with a roller ensured even spreading of the material across the mold. In a later version of the technique, an additional sacrificial layer improved particle recovery [100]. This adhesive layer was designed to adhere to particles, but not to PFPE, and helped with unmolding of the cured features. The layer was disrupted later on, in order to release the monodisperse particles into solution. The applications of the PRINT technique, however, have mainly focused on high resolution production of nanoparticles dedicated to drug delivery and nanomedicine [101].

Other groups applied similar replica molding techniques to produce larger hydrogel microparticles for biosensing. For example, the Yi group demonstrated the polymerization of a PEG substrate [37], as well as of a hybrid material of PEG and chitosan [48,49], into particles in PDMS microwells. Particles were shape-encoded and functionalized with oligonucleotides (Fig. 4d). PDMS molds were patterned using silicon wafers, through standard soft

lithography methods. The mold was filled with monomer, cleared of excess solution and air bubbles, and sealed with a PDMS-coated glass slide, leaving a small air gap above monomer layer. It appeared necessary to assemble the device in a high humidity controlled chamber to prevent monomer evaporation. Indeed, in ambient conditions, the 400 pl volume per well rapidly evaporated, resulting in gel non-uniformity and variable DNA density within the material. This technique enabled production of 1600 particles per batch with a minimal use of monomer (100 μl for 100 batches, assuming that excess monomer was recovered at each step). Particle recovery, however, required multiple steps of physical bending of the mold and re-suspension of particles on the mold surface through pipetting.

3.3. Droplet-based synthesis of spectrally encoded spherical particles

While lithographic techniques are used to generate graphically encoded hydrogel microparticles (extruded or shape-encoded), spherical spectrally encoded gel beads can be synthesized using water-in-oil droplet-based synthesis systems. Most platforms are based on microfluidic techniques for generating monodisperse and stable aqueous droplets in an immiscible oil phase. These innovative techniques have been reviewed extensively elsewhere [13,31,102–106]. Here, we focus more specifically on applications to crosslink droplets of photocurable or chemically crosslinkable monomers into hydrogel beads.

Hydrogel bead arrays are typically generated by optically encoding the spheres using a range of techniques. By choosing biofriendly monomers such as PEGDA or alginate, researchers have been able to crosslink these droplets in situ upon formation in the microfluidic device, load them with dyes or quantum dots, and/or functionalize them with biomolecules for biosensing applications. PEG-based monomers can be crosslinked using UV exposure whereas alginate is chemically cross-linked using introduction of calcium or barium ions. Although some of the studies reviewed below do not demonstrate biomolecule immobilization in the particle yet, the innovative encoding routes they report are attractive candidates for future multiplex bioassay development.

3.3.1. Droplet formation using T-junctions

A common geometry employed in synthesis of droplet-based hydrogel beads is the T-junction. The aqueous dispersed phase meets the continuous-phase at a cross-junction where droplets are pinched off. Stream flow-rates and device dimensions control the droplet formation rate and size. For example, Kantak et al. used a microfluidic T-junction and UV induced photopolymerization to generate PEG spheres with a 72 μm diameter (Fig. 6a) [39]. The spherical particles contained fluorescein isothiocyanate dextran (FITC-dextran) and a sugar binding protein for a fluorescence-based glucose detection assay. Others reported the use of a T-junction made of PTFE tubing for the fabrication of 300–400 μm photonic crystal hydrogel beads. PEGDA was mixed with a suspension of with silica nanoparticles (similar encoding method as Ye et al. [50]). Droplets of the mixture were dispersed in oil and UV-polymerized [107,108].

The simplicity of the T-junction has led to its use in combination with other microfluidic techniques for fabricating particles with higher complexity. Gerver et al. combined a microfluidic herringbone mixer with a T-junction scheme to synthesize spectrally encoded 46 μm PEGDA spheres with mixtures of down-converting lanthanide nanocrystals [40]. Prior to the T-junction, three input streams were separately fed into the device. Each one contained PEGDA, a photoinitiator, and different lanthanide nanophosphor. Streams were mixed on the herringbone mixer. Precise pressure control on these streams was used to program the relative ratios of nanophosphors. The monomer mixture was then pushed into the T-junction using a high-pressure water stream for droplet formation. Finally, droplets were exposed to UV light and crosslinked into hydrogel beads entrapping nanophosphors (down-converting lanthanide nanoparticles) inside particles (Fig. 4i). The input stream ratios could be adjusted before each bead synthesis, providing an easy route to generating uniquely encoded beads in a single device. The study demonstrated the generation of 24 unique codes that were read out with high precision. However, by increasing number of lanthanide nanophosphor inputs (potentially up to 14), the multiplexing capability could be significantly increased.
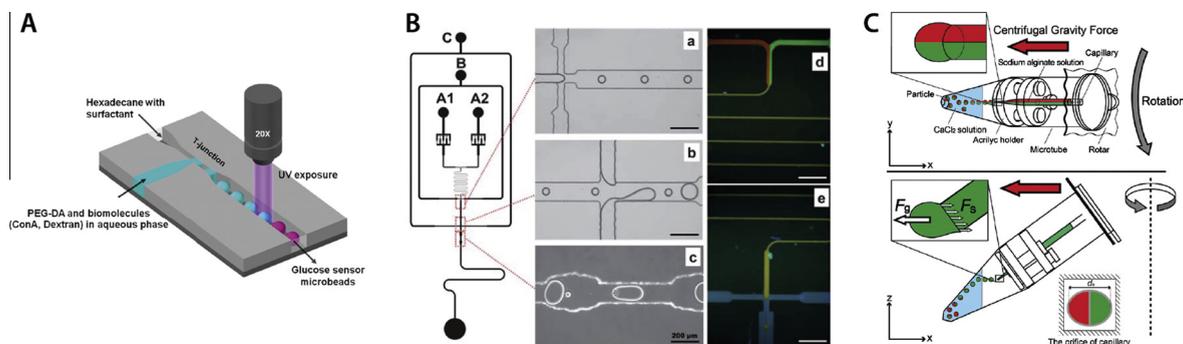
Fig. 6. Droplet and centrifugal force-based approached for particle synthesis. (A) Fabrication of PEG microbeads using T-junction geometry: droplets of monomer are formed at the T-junction and are crosslinked with UV exposure. Reproduced from [39]. Copyright 2012 AIP. (B) Fabrication of alginate microparticles using a combination of flow-focusing and T-junction geometries in a microfluidic device: gelation occurs in a fusion chamber and QD-doping is visible under fluorescence. Reproduced from [65]. Copyright 2011 RSC. (C) Centrifugal synthesis of alginate microspheres using multibarrel capillaries: alginate microdroplets fall into a solution of CaCl2 and gel upon contacting the solution. Reproduced from [54]. Copyright 2012 Wiley.

3.3.2. Hydrodynamic flow-focusing for droplet synthesis in conjunction with T-junctions

In a flow-focusing device, hydrodynamic focusing is used to generate emulsions of the dispersed aqueous phase (such as the monomer solution) into a sheath stream of the continuous oil phase. The droplets are pinched off into the continuous phase. Based on the dimensions of the device and the flow-rate of the dispersed phase, there is full control over droplet size and rate of droplet formation.

One study combined a flow-focusing scheme with a double-T-junction to synthesize quantum-dot encoded alginate particles with a 25–30 µm diameter [53,65]. The flow-focusing geometry was used to generate stable alginate droplets in the continuous phase (soybean oil), while the T-junctions were used to introduce the barium ions necessary to crosslink the alginate matrix in a fusion chamber (Fig. 6b). CdSe/ZnS quantum dots (QD) added to the monomer solution beforehand were eventually encapsulated in the final hydrogel particles. The authors demonstrated the ability to create different codes by changing the ratio of alginate to QD solutions in the inlet (Fig. 4j). By using a long wavy channel, these streams were then allowed to mix before being injected into the soybean oil, providing the capability to make up to 100 codes using only two QD colors. The QD-doped particles were further functionalized with an antibody through non-covalent adsorption and were used in IgG detection assays.

Another study reported the use of a similar double T-junction combined with a flow-focusing scheme to produce alginate beads loaded with glucose oxidase, for glucose sensing applications [109].

3.3.3. Capillary microfluidic devices

An alternate strategy for droplet formation uses coaxial capillaries. The dispersed phase flows through the inner injection capillary, while the outside capillary contains the continuous phase, resulting in droplet formation at the tip of the injection capillary. The Weitz group developed complex microfluidic geometries for generating QD-tagged gel spheres through double emulsion polymerization [110]. The authors used a capillary microfluidic device utilizing both co-flowing streams and a flow-focusing geometry to polymerize double emulsions containing quantum dots in the innermost droplet and PEGDA in the outer shells. PEGDA hydrogel shells (diameter ~200 µm) were generated with UV illumination, entrapping 50-µm QD inside the resulting particles. Using only two quantum dot colors at 30 levels, the technique could provide up to 899 codes. The double emulsion technique was also used to make the resulting particles magnetic for easy post-processing and collection.

Similarly, Cheng et al. designed a capillary microfluidic device to generate anisotropic encoded particles from a PEGDA precursor containing colloid crystals [111]. Right after formation, droplets were captured in an anisotropic collection capillary of smaller cross section. Droplets were squeezed into a rectangular or square collection capillary, forcing them into anistropic shapes, and photopolymerized in situ.

3.3.4. Centrifugal synthesis

In parallel to aforementioned microfluidic chip-based techniques, two recent studies take advantage of centrifugal forces to synthesize complex multi-compartmental spherical alginate particles [54]. Both studies use modified microtubes to perform centrifugal synthesis. Fig. 6c depicts the typical device used. Two physically separated compartments contain an alginate solution (top) and a calcium ion solution (bottom). An ejection system makes the liaison between the top and bottom compartments. Placed in a centrifuge (simple bench top system) and rotated, the alginate mixture is pushed down through the ejection system by the centrifugal force, eventually forming a droplet at the interface between air and liquid. If the rotation is fast enough, the centrifugal force overcomes the interfacial tension effects, resulting in the droplet ejection. Physical crosslinking of the droplet is immediate upon entry into the solution containing calcium ions. The resulting gelified particles are monodisperse and their size can be adjusted with the centrifugal force while their shape (sphere or ellipse) depends on the distance between the tip and the surface of calcium ion solution. The alginate precursor can be mixed with biological species to be incorporated in the structure. Moreover, using multiple capillaries, two (or more) alginate solutions can be co-injected as laminar flows to form Janus particles.

Using an ejection system based on multiple glass capillaries fixed in an acrylic holder, Maeda et al. demonstrated the fabrication of multiphasic hydrogel particles with up to six-compartment body compositions [54]. The authors separately encapsulated magnetic nanobeads and cells in 2-compartment spheres. Lee et al. used a needle-based droplet ejection system to fabricate 250–750 µm complex alginate particles embedded with sensory polydiacetylene liposomes for the colorimetric detection of melamine, a chemical with kidney toxicity [55] (Fig. 4k). Biphasic and triphasic particles were also produced using co-injection of monomer solutions of various formulations. This simple process, which operates in mild conditions (no oil, heating or UV light) with a simple equipment, appears particularly well-suited for the capture of sensitive biological materials such as cells and liposomes into hydrogel particles.

4. Processing particles and reading the code

A major advantage of suspension arrays in comparison to planar arrays is the possibility to mix particles thoroughly in the sample or washing solution and to overcome diffusion constraints during incubations. However, it is necessary to develop strategies for washing and collecting particles at multiple steps of the assay protocol without particle loss. Similarly, methods for analyzing the code and target level for each particle individually should be designed.

4.1. Mixing and washing particles

4.1.1. Passive manipulation

Different assay formats have been reported depending on the specific requirements of the application

(throughput, end-user). Hydrogel particles assays have been performed in microtubes (50–500 µl) [70–72], in microplates (50–500 µl) for higher throughput [51], and in microfluidic devices (<10 µl) for low volume applications [34,38]. For all of these scenarios, it is necessary to establish efficient techniques for particle mixing, washing and collection.

In tubes or microplates, particles can be separated from the supernatant using centrifugation. Once particles form a pellet at the bottom of the vial, the supernatant is removed and particles are re-suspended in fresh washing buffer. Alternatively, Appleyard et al. proposed a protocol for performing a hydrogel-based immunoassay in a hydrophilic low protein-binding filtration microplate (polyvinylidene fluoride membrane) [51]. Rinses were performed using vacuum suction, and the 250-µm barcoded particles were large enough to be retained by the 1.2 µm filter membrane using vacuum rinse steps (although we note that excessive suction can induce deformation). Incubation and rinsing steps could thus be performed in a single well.

In microfluidic devices, it is necessary to trap particles during buffer exchange steps and during introduction of new reagents to avoid particle loss (for general reviews on particle or bead handling in microfluidic devices see [82,112]). Choi et al. developed a microfluidic chip that combines a polymerization chamber for particle in-situ fabrication and a reaction chamber to perform the assay and to read the particle output [34]. To capture particles, the authors included pillars at the end of the reaction chamber, as a filter (Fig. 7a). Trau and coworkers reported a strategy for capturing cylindrical sensing particles

(50 µm diameter) on a gel well array in a microfluidic chamber [66]. To form the particle array, the solution of sensing PEG-based particles was dispensed on the gel well array. Some particles settled in wells and remained immobilized in gel wells merely through physical entrapment for the entire duration of the assay. Meanwhile free particles were easily rinsed off. Notably, similar techniques of particle docking in well arrays have been recently reported by the Sia group for docking particles based on their shape [113] and by the Kwon group for creating arrays of spectrally encoded gel beads [114].

4.1.2. Active control using magnetic particles

Magnetic microbeads can be entrapped inside a tightly crosslinked hydrogel at the time of the gel polymerization. These embedded entities confer magnetic properties to the resulting sensing particles and offer a way to orient and transport them. Bong et al. demonstrated that the incorporation of superparamagnetic beads on one end of barcoded sensing particles generated magnetically addressable particles that were responsive to weak magnetic fields. There was no interference with the assay sensitivity or specificity [68]. Using a magnet, particles could be efficiently separated from bulk solutions for washing steps and could be oriented for imaging. In a subsequent paper, Suh et al. used magnetic tweezers to transport and array such particles inside microwells for imaging [115].

Lee et al. reported precise multi-axis rotational control over particles made using a color tunable magnetic material through an external magnetic field [38]. The particles were dedicated to a DNA hybridization assay in a low
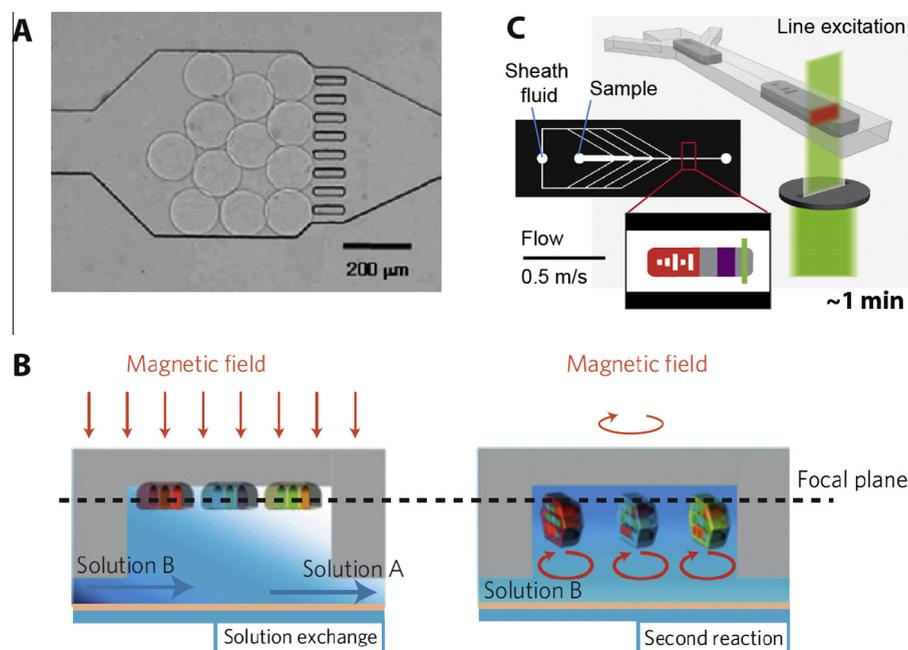
Fig. 7. Particle processing techniques. (A) Fabrication of PDMS microposts inside microfluidic device to retain gel particles through rinsing and assay steps. Reproduced adapted from [34]. Copyright 2008 Springer. (B) Use of magnetic fields to manipulate particles that are doped with magnetic entities: direction of field can be exploited to either make particles align along an axis or continuously rotate in solution. Reproduced from [38]. Copyright 2010 NPG. (C) Microfluidic cytometer used to decode and analyze graphically encoded gel microparticles: reading throughput is up to 50 particles/s; sheath flows and sharp contractions in the device lead to alignment of particles into single file as they cross the detector. Reproduced from [51]. Copyright 2011 NPG.

volume chamber. For buffer exchange or imaging steps, the external magnetic field was applied to trap particles in the micro-chamber, forcing them to lay flat and in a specific 2D orientation (Fig. 7b). On the contrary, during the incubation and washing steps, particles were continuously rotated on the vertical axis, thereby creating local microscale rotating stirrers.

4.2. Detection and signal acquisition

As for the majority of bead-based assays, reading the code and quantifying the target reporter signal on hydrogel particles can often rely on optical detection methods (for general reviews on bead-based array decoding see [83,112,116,117]). Two approaches have been reported for signal acquisition: imaging methods [33,34,37,38] and flow cytometry-like scanning techniques [44,69]. It is critical to use non-interfering methods for decoding the array and for target level quantification and to make sure that both readouts are easily de-convoluted from each other. Examples of non-interfering readouts are: orthogonal fluorescence reporters [65], spatially-separated code and target regions [38,55,69], or shape-encoding in combination with a fluorophore signal reporter [33,34,118].

4.2.1. Imaging particles

The majority of strategies for decoding hydrogel particles rely on imaging techniques. Transmission, reflection, or fluorescence microscopy is used to image the structural color of particles [38,50] or their spectral signature when encoded with fluorophores [33,37,69], quantum dots [65], up-converting nanoparticles (excited in near IR) [81], or down-converting nanoparticles (excited in deep UV) [40]. For graphical encoding in particular, imaging enables capture of complex information about the particle shape or bit-code (extruded regions) in a single acquisition. However, examples of automated particle decoding based on image analysis are rare [119] and decoding is often manual.

For a reliable and faster decoding process, it is often necessary to orient particles before imaging. High aspect ratio shape-encoded or barcoded particles tend to fall flat when dropped and sandwiched on a glass slide, making it easier to image them in 2D. In addition, magnetic particles can also be oriented in 2D and aligned using an external magnetic field (Fig. 7b) [38,115]. Particles can also be trapped in microfluidic devices, one example is in a filtering chamber (Fig. 7a) [34]. Another method is to trap them as a single line of particles in a narrow microfluidic channel (Fig. 4g) [40].

4.2.2. Scanning particles

The Doyle group developed a microfluidic scanner dedicated to the high-throughput analysis of barcoded hydrogel particles [51,69] (Fig. 7c) The sensing particles display a tablet-like shape and are typically composed of four sections: a graphically encoded fluorescent head with internal holes and a probe functionalized tail for target capture, flanked by two inert spacing regions. For analysis, particles are fed into a flow-focusing microfluidic channel with several contractions. Side sheath streams orient the

tablets with the flow at the center of the channel [44]. The well-ordered particles then pass through a thin excitation beam generated by focusing a laser beam through a slit, and the fluorescence signal is integrated on the portion of particle passing through the detection zone. The fluorescence profile of the entire particle is automatically reconstructed from the multiple data points acquired per particle. The holes in the code region generate a unique fluorescent signature and enable determination of the particle orientation in the flow (code region or probe region first). Indeed, for anisotropic particles, assessing the particle orientation and position at the time of the analysis is often a challenge [83]. Using a similar principle, the company Firefly™ BioWorks developed a particle array based on 1D-barcoded particles, that can be read using conventional benchtop cytometers [120]. Particles are used in miRNA multiplex detection assays. Currently, up to 68 miRNA targets can be analyzed simultaneously in a sample.

Notably, scanning detection techniques can be advantageously coupled with microfluidic particle sorting techniques. Thus, Tumarkin et al. used a flow-cytometer coupled with a microfluidic sorter to sort cell-laden agarose particles in a high-throughput combinatorial cell co-culture screen [121]. Hydrogel sensing particles could similarly be separated and collected selectively, based on the assay outcome or on the particle code.

5. Multiplex biosensing on hydrogel particle arrays

In this section, we review the applications of hydrogel particles to biosensing assays reported in the literature to date. We focus here on the assay design and performance (multiplex encoding and decoding strategies are detailed in Sections 3 and 4 respectively). Table 2 compares the main characteristics of these nucleic acid detection assays, immunoassays, and enzymatic assays. Fig. 8 summarizes the different strategies used for target capture and reporting. Notably, all assays reported so far rely on optical methods generally utilizing fluorescent reporters.

5.1. Nucleic acid detection

5.1.1. Oligonucleotide

5.1.1.1. Direct hybridization assay. Shape-encoded PEGDA hydrogel arrays were used in 2004 by Meiring et al. for nucleic acid sensing [33]. In these assays, particles were functionalized using methacrylamide-modified oligonucleotides. The authors demonstrated the detection of three different target sequences, labeled using different fluorophores (Fig. 8a). The authors were also able to show specific detection of single nucleotide polymorphisms (SNPs). Since that time, multiple other types of hydrogel particles have been used for nucleic acid detection.

Stop-flow lithography-synthesized hydrogel particle arrays have been used and optimized extensively for nucleic acid detection. In 2007, Pregibon et al. synthesized multifunctional graphically encoded particles that were covalently functionalized with acrylate-modified DNA probes [69]. The particle array was hybridized with
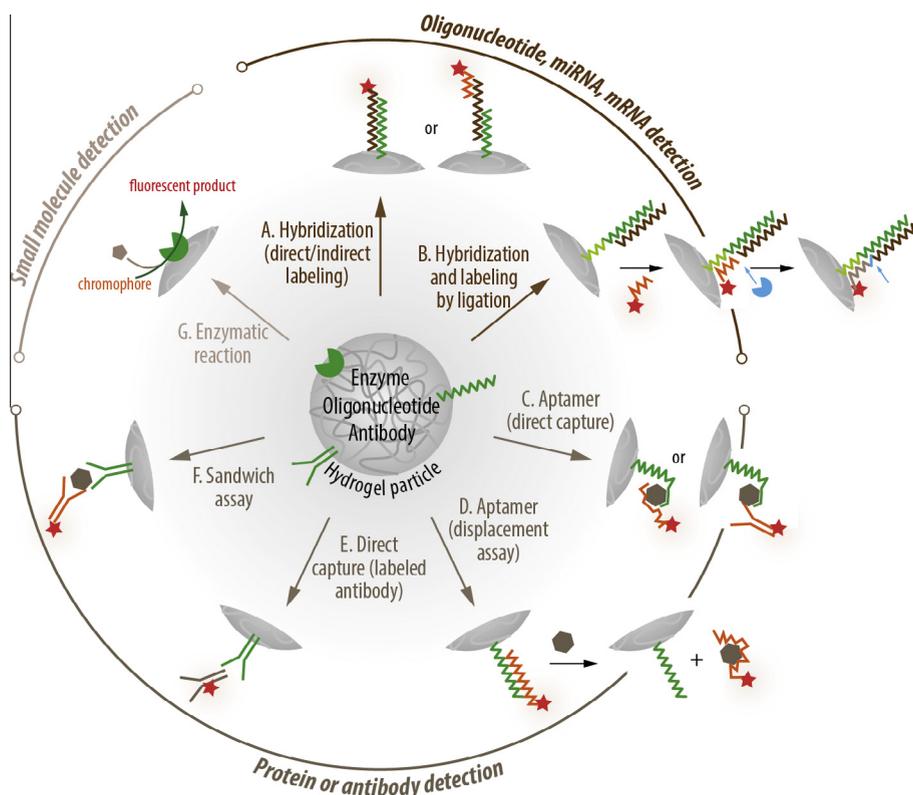
Fig. 8. Bioassays on hydrogel particles. Various methodologies used to functionalize gel particles with biological entities and quantitate analytes in solution reported in the literature: A [33,35,37,38,45,69,107,108,111], B [70,92], C [71], D [50], E [65,74], F [51,72], G [66,67,109]. Three classes of molecules that have been detected using gel particle arrays: oligonucleotides (using hybridization and/or ligation labeling techniques), proteins or antibodies (using sandwich or competition assays), and are small molecules (using enzymatic sensors).

complementary fluorescent DNA targets. The authors demonstrated high assay specificity and functionalized individual chemically anisotropic single particles with more than one DNA probe, allowing for multiplexing on the same particle. A 2009 study further optimized these particles and showed single-attomole DNA detection using two types of fluorescent markers (streptavidin phycoerythrin and PicoGreen®) [35].

In 2010, Lee et al. demonstrated the use of color-coded magnetic polymeric microparticles for use in DNA hybridization assays using a variation of flow lithography, demonstrating the specific detection of two different nucleotide target sequences [38]. Additionally, the authors showed that magnetic mixing enhances reaction kinetics significantly in the same reaction time period relative to running the hybridization assay on stationary particles.

Meanwhile, Lewis et al. examined the use of shape-encoded PEG-DA hydrogel particles fabricated using replica-molding for oligonucleotide sensing as well [37]. Three different fluorescently-labeled DNA sequences were used to demonstrate specificity and sensitivity of the assay. The assay demonstrated a limit of detection of ∼10 pM with linear signal from 10 pM to 100 nM. Finally, the Gu group demonstrated proof-of-concept hybridization assays on PEG particles synthetized using microfluidics and encoded with photonic crystals [107,111,122].

5.1.1.2. Alkaline dehybridization assay. Zhang et al. demonstrated the use of hydrogel particles generated via stop flow lithography for SNP discrimination using alkaline dehybridization [123]. In these assays, spatio-optically-encoded particles contained probes for two different allele-specific oligonucleotides that differed by a single nucleotide. The particles were annealed with fluorescent targets. Duplex dehybridization was then induced via alkaline stimulus in the form of either a pH step function or a temporal pH gradient. Fluorescence microscopy allowed the characterization of signal change over time, which accordingly provided information about the kinetics of the dehybridization process. Using the pH gradient the method provided data about dehybridization rate over a large temperature range for targets with different SNP insertion points. This result was particularly significant for being able to identify SNPs closer to the end of a DNA strand. Furthermore, the authors applied the assay to the detection of clinically relevant SNPs in thrombotic disorders. The authors successfully identified the samples' genotypes.

5.1.2. microRNA (miRNA)

In 2011, Chapin et al. developed a novel universal labeling system for microRNA detection on gel particles [70]. In contrast to protein detection assays, in which one can employ a gel-embedded capture antibody for target

capture and a detection antibody for target labeling, nucleic acids do not offer several epitopes. Chapin's approach made use of a microRNA probe with two distinct binding regions: one for the miRNA target and one for the universal label. Fig. 8b describes the assay workflow. Hydrogel particles were incubated with the sample first, and then with the universal label. When both the target sequence and the biotinylated universal label were hybridized on the probe, an enzymatic ligation step linked the universal label to the bound miRNA target. Finally, the complex was labeled with a fluorophore through the biotin group.

This concept of using a universal linker to label the bound targets eliminates the need for pre-labeling of the targets. Additionally, this approach does not introduce target-based biases like PCR-based approaches do. The universal linker in this study was further used to develop a signal amplification scheme using rolling circle amplification [92], where the miRNA target was bound to the probe and the amplification that occurred was based on the universal linker, rather than the target, once more eliminating bias. Sub-femtomolar concentrations of miRNA could be successfully detected in complex samples, with an overall detection range expanding over six orders of magnitude.

5.1.3. mRNA

Nucleic acid laden particles were also developed for the detection of longer mRNA sequences. Choi et al. demonstrated that it is possible to increase overall particle porosity by altering the porogen in the PEG particles, allowing diffusion of larger nucleic acids such as mRNA while preserving the same degree of probe functionalization [45]. The porosity-adjusted particles were functionalized with short probe sequences and reacted with capture extenders to enable capture of the mRNA target. The targets were then labeled using a mixture of label extenders specific to each target. All the extenders bore a similar universal labeling region that was biotinylated (with one or several biotins for signal amplification). The complexes were finally labeled using a streptavidin-conjugated fluorophore. The authors demonstrated up to 6.4 amol detection limit using a universal adaptor with multiple biotins, which was comparable to commercial bead-based assays.

5.2. Protein/antibody sensing

Given the need for multiplexed tests in the biomarker analysis field, parallel efforts have focused on adapting traditional immunoassays to hydrogel particles for protein or antibody detection. First, the traditional antibody-linked sandwich assay was successfully transferred to a multiplex particle-based format by immobilizing antibodies into hydrogel particles [51]. Recent reports explore aptamer-based strategies for innovative protein sensing on hydrogels [50,71]. Multiplexed immunoassays are usually more complex to develop than nucleic acid sensing assays. Indeed, proteins are fragile biological entities, reagent reproducibility is low, and frequent cross-reactivity and non-specific binding issues are often encountered.

5.2.1. Antibody-based capture of protein

5.2.1.1. Sandwich assay. The first immunoassay on hydrogel particles, and most advanced one so far, was reported in 2011 by Appleyard et al. [51]. The authors developed a complete sandwich immunoassay for multiplexed detection of cytokines on barcoded PEGDA particles. The assay was successfully applied to the detection of a panel of three cytokines involved in immune response signaling: interleukin-2 (IL-2), interleukin-4 (IL-4) and, tumor necrosis factor alpha (TNFα) [72]. Three sets of particles with unique barcodes were functionalized with antibodies against the three proteins and were pooled in the sample. The captured targets were sandwiched between the immobilized probe antibody and a secondary biotinylated reporter antibody (Fig. 8f). Streptavidin–phycoerythrin conjugates enabled generation of fluorescent reporter signal. Target samples were spiked in with fetal bovine serum (FBS) in order to mimic the complexity of biological samples. The bio-inert PEG hydrogel did not collect non-specific signal in these complex samples, avoiding the need for prior purification of the sample.

Single-plex calibration studies demonstrated a 3-log dynamic range for each target and low limits of detection comparable to gold standard ELISAs (8.4 pg/ml for IL-4 and down to 1.1 and 2.1 pg/ml for IL-2 and TNFα; calculated as three standard deviations greater than the control). These results were compared to two commercial multiplex assays. First, the hydrogel particles clearly demonstrated an improved sensitivity compared to the reference planar array based-assay, without any signal amplification. Additionally, limits of detection ranged in the same order of magnitude as detection limits reported for the Luminex® bead-based assay. The Luminex® assay, however, required higher number of bead replicates for statistical purposes and additional filtration steps.

Multiplexing studies successfully demonstrated the simultaneous detection of the three targets in a single sample, in both an interplex format (one probe per particle, three particle types) and an intraplex format (a unique particle type with three chemical probe regions). Target detection was selective, quantitative recovery of the FBS spike-ins ranged within 20% of predicted values from the calibration curves, and no significant cross-reactivity was observed.

5.2.1.2. Direct antibody capture. Two proof-of-concept studies demonstrated the direct detection of target antibodies on different antibody-functionalized hydrogel particles (Fig. 8e). In 2012, Park et al. functionalized shape-encoded PEGDA particles with mouse IgG and IgM antibodies [74]. Particles were engaged in a two-plex assay for the direct capture of FITC-labeled anti-mouse IgG and IgM target antibodies. Targets were detected selectively with a linear correlation between the fluorescent signal and the target concentration in the tested range (up to 500 ng/ml; no LOD determined).

The second study featured alginate beads [65]. In 2011, Ji et al. demonstrated a proof-of-concept immunoassay on alginate particles functionalized with anti-human IgG antibodies through non-covalent adsorption. A 2.2 mg/ml limit of detection was demonstrated for a FITC-labeled human

IgG target, with a linear correlation between the fluorescence signal and the target concentration from 5 to 40 mg/ml (plateau at 60 mg/ml). Particles were blocked with bovine serum albumin (BSA) to prevent non-specific binding, but no complex sample was tested. Although no multiplexed study was performed, the particles were encoded with a mixture of two quantum dots (λ_{em} 570 nm; 613 nm). It appeared, however, that the red tail of the FITC target reporter signal overlapped the 570 nm QD signature, hence potentially interfering with target quantification.

Finally, Yang et al. reported a strategy to detect tumor markers on encoded silica–hydrogel hybrid beads through a non-competitive immunoassay [124]. Labeled reported antibodies are incubated with the sample as well as particles functionalized with the protein of interest. Higher amounts of targets in the sample capture more reporter antibodies in solution, resulting in a decreased signal on the particles. Calibration curves were obtained for two markers (pure solutions of target proteins; 1 ng/ml to 0.1 mg/ml).

5.2.2. Aptamer-based capture of protein
5.2.2.1. Aptamers.
Recent studies have explored aptamer–based sensing approaches for the detection of proteins on hydrogel particles array [50,71]. Aptamers are short single-stranded nucleic acid sequences designed and engineered to bind to a target of interest with high affinity and selectivity. Aptamers are selected through an iterative *in vitro* selection process called SELEX (*systematic evolution of ligands by exponential enrichment*). With dissociation constants in the low-nanomolar range, low cross-reactivity, better stability and reproducibility, aptamers have gained increasing attention as an attractive alternative to antibodies as affinity agents for biosensing applications [125]. Due to the existing knowledge base in the field built around DNA multiplexed assays, aptamers can be readily modified, and integrated into microarrays, bead-based assays, as well as amplification schemes. The secondary structure of aptamers, though, is particularly sensitive to the assay conditions such as the ionic environment. As the structure is critical for target binding, assay optimization can be challenging.

5.2.2.2. Sandwich assay.
In 2011, Srinivas et al. reported an α-thrombin detection sandwich assay using an aptamer probe embedded in barcoded PEGDA particles [71]. Two strategies were simultaneously evaluated for the reporter molecule: a second reporter aptamer sequence or a specific reporter antibody (Fig. 8c). Both reporters were biotinylated to enable the subsequent labeling of target capture events with streptavidin–phycoerythrin conjugates. By optimizing buffers, the authors achieved limits of detection in the picomolar range (respectively 21.7 pM and 4.09 pM), surpassing standard non-amplified surface-based assay for thrombin. Additionally, an excellent assay reproducibility was observed (CV < 10%). Using two sets of barcoded particles, the authors demonstrated the ability to simultaneously measure thrombin and IL-2 for both aptamer and antibody-based detection and showed minimal interference from background proteins such as BSA and IgG. A

mixture of proteins with structures similar to α-thrombin was used to assess specificity with regard to thrombin subtype. Specificity assays were successful for the aptamer/aptamer sandwich, but failed for the aptamer/antibody system.

5.2.2.3. Displacement assay.
In 2011 also, Ye et al. reported a displacement assay for aptamer-based protein sensing in PEG hydrogel particles [50]. In this approach, the hydrogel particle was functionalized with an oligonucleotide sequence complementary to the aptamer probe. Particles were initially saturated with the aptamer probe. The aptamer probe was labeled with a fluorophore (Cy3), so that the particles were initially fluorescent. In presence of the target protein, however, the aptamer was released from the particle and preferentially interacted with the protein (Fig. 8d). As a result, the particle fluorescence decreased. The signal decrease correlated to the concentration of target in the sample.

The authors demonstrated selectivity for the multiplex detection of three targets: adenosine, thrombin, and IgE. A unique combination of shape (graphical code) and structural color (photonic code) was used to encode particles for a 3-plex assay. Buffers were optimized to maximize the fluorescence shift upon target binding and minimize the cross-reactivity between capture/target pairs. A dose–response curve for adenosine detection demonstrated a dynamic range from μM to mM concentrations, along with a good reproducibility (CV (inter particles): 2.2%; CV (inter assays): 4.7% ($n = 5$)).

5.3. Enzymatic sensors

A few reports investigated the synthesis of enzyme-immobilized hydrogel microparticles and their ability to sense small molecule analytes such as glucose [66] (Fig. 8g). For example, in a 2008 study by Lee et al., both glucose oxidase (GOx) and horseradish peroxidase were physically entrapped into PEG hydrogel particles [67]. Particles were pooled in samples along with Amplex® Red molecules. GOx units reacted with target glucose molecules, releasing hydrogen peroxide. In turn, hydrogen peroxide molecules were subsequently consumed by HRP to convert Amplex® Red molecules into fluorescent resorufin. The fluorescent product then remained in the gel in a dose-responsive manner. The authors examined glucose concentration over the range of 0.1–10 mM. The authors have also shown the ability to run similar reactions using alkaline phosphatase as the enzyme and FDP as the substrate. In these assays, the fluorescent product emits at a different wavelength, opening up the possibility of running multiplexed enzyme assays.

Polymerized PEG droplets were also used to run glucose detection assays by different groups. In 2012, Kantak et al. synthesized PEG spheres that contained fluorescein isothiocyanate dextran and tetramethyl rhodamine isothiocyanate conjugated concanavalin A (TRITC-ConA), a sugar binding protein [39]. The TRITC-ConA acted as a quencher, reducing fluorescent signal in the presence of the fluorescein-dextran conjugate. However, since glucose has a higher affinity for ConA than dextran, upon introduction of

glucose, the FITC-dextran was released from the TRITC-ConA, providing signal increase proportional to the amount of glucose. The authors demonstrated a linear relationship between resulting fluorescent intensity and glucose concentration between 1 and 10 mM. In addition to PEG, glucose oxidase functionalized alginate droplets have been used for glucose detection in a study by Um et al. in 2008 [109].

6. Perspectives

The field of hydrogel particles for sensing has progressed significantly since the first demonstration of hydrogel substrates as scaffolds for biosensors. For example, the microRNA gel particle kit sold by Firefly™ Bioworks now can profile 68 microRNAs directly in clinical samples, such as total RNA and cell lysate. The technique is compatible with several commercially available cytometers, and has been used to generate biologically relevant data in prominent fundamental research studies [126]. Such examples of translation of a proof-of-concept into a fully developed product remain, however, limited. Although there has been tremendous development in fabrication and encoding techniques, a survey of the literature shows that often, platforms are lacking in development of companion technologies to enable analysis of particles after assay with sufficient throughput or automated solutions. Additionally, particle performance has not always been gauged in real clinical samples. Moreover, though many technologies have high multiplexing capacities in theory, usually only 2–3 targets were measured at once, which may not be representative of a real clinical setting. For this field to continue advancing, it is necessary to take other reported innovative advances in gel particle synthesis and enable their clinical integration forward from current proof-of-concept applications. Given the clearly high potential of hydrogel particle arrays for biomolecule quantification, these benchmarks should be a priority in assay design and optimization.

Furthermore, the majority of the work discussed in this review used fluorescence-based detection methods for target quantification. However, it is also possible to use label-free sensing on gel particles as shown by the Gu group [122,127]. In future work, it should be also possible to integrate other types of label-free sensing methods with hydrogel particles or to leverage the potential of stimuli-responsive gels for sensing [128]. A recent paper reported the use of temperature-responsive poly(N-isopropylacrylamide) particles in conjunction with an electrochemical luminescence amplification method [129]. Hydrogel microlenses were fabricated from poly(N-isopropylacrylamide-co-acrylic acid (pNIPAAM) for label-free sensing using differential interference constrast imaging [130], and microlens particles were produced using stop-flow lithography [131]. Combined with detection techniques and biomolecule immobilization strategies, these novel chemistries could open new avenues for target detection on gel particle arrays.

Another application of stimuli-responsive pNIPAAM gel particles is protein or analyte concentration using "high-affinity baits" embedded in the gel matrix [132,133]. The "bait" can be a charged molecule or a functional group that encourages proteins to enter the gel matrix. The defined gel pore size enables to control the size of target molecules that diffuse in, hence selecting proteins of only a certain size. The same concept of bait molecule is used in pull-down assays on agarose gel beads, in order to study physical interactions between two or more proteins (Thermo Fisher Scientific [134]). The agarose gel is pre-functionalized with an affinity ligand which can later capture a tagged protein as interest. That protein is used as a bait to capture interacting proteins in biological samples. Interacting complexes can be eluted and analyzed. On a different note, biological gels composed of DNA or proteins are interesting for sensing applications. Bulk studies using DNA-based aptamer gels or single-stranded DNA gels that can be structurally switched have yielded promising results for sensing of proteins [135,136]. These concepts truly take advantage of the various advantages of tunable hydrogels and could be translated to a particle array format in future work.

Looking forward, we foresee significant opportunity for single cell sensing using hydrogel microparticles. Single cell characterization is of notable recent interest due to heterogeneities in cell populations, implying that that measuring analytes on a bulk scale from cell cultures or from cell lysates may not provide a full picture of cell behavior in various diseases or settings. Rather, looking at single cell secretion tendencies or response to stimuli would lead to better understanding of biological processes that accounts for intrinsic population variation [137]. However, such studies require the analysis of up to thousands of cells to generate statistically significant data. Thus far, microfluidic technologies appear as a promising technology for single-cell analysis, but these endeavors have required significant fluidic optimization and are still being developed [138]. For example, it is now possible to achieve encapsulation of a single cell per droplet using droplet-based microfluidics [139]. Alternatively, others have encapsulated single cells in microwells and analyzed secretion of proteins over time [140]. There has also been a parallel effort towards the creation of novel device geometries for high throughput single-cell analysis [141,142].

We expect that hydrogel particles could additionally be a valuable and particularly unique tool for single-cell encapsulation and subsequent analyte profiling, and could be interfaced with some of the technologies mentioned above. Importantly, the hydrogel chemistries discussed in this review are biocompatible and non-fouling and can be readily functionalized. In contrast to water droplets, the gels themselves could be functionalized with probe molecules to capture single-cell secreted analytes. Significant effort has been devoted to developing strategies for immobilization of cells and creation of co-cultures in three-dimensional hydrogel scaffolds and even particles [7,87,143–145]. For example, PEGDA beads were recently synthesized using droplet microfluidics and used to create micro-cultures of liver tissue [146]. Other droplet-based systems were able to successfully trap cells into alginate or agarose gel microparticles in proof-of-concept work [62,121,147–149]. Flow lithography was used to capture

cells inside PEG microparticles [150], and to create free-flowing cell-containing complex microcarriers [97]. Although several groups have indeed begun to investigate fabrication techniques for single-cell encapsulation, analytical measurements have not yet been made on such hydrogel arrays. Development of gel particles for single-cell sensing will be very promising in future applications.

Acknowledgments

References

[1] Langer R, Tirrell DA. Designing materials for biology and medicine. Nature 2004;428(6982):487–92. http://dx.doi.org/10.1038/nature02388.

[2] Rubina AY, Kolchinsky A, Makarov AA, Zasedatelev AS. Why 3-D? gel-based microarrays in proteomics. Proteomics 2008;8(4):817–31. http://dx.doi.org/10.1002/pmic.200700629.

[3] Helgeson ME, Chapin SC, Doyle PS. Hydrogel microparticles from lithographic processes: novel materials for fundamental and applied colloid science. Curr Opin Colloid Interface Sci 2011;16(2):106–17. http://dx.doi.org/10.1016/j.cocis.2011.01.005.

[4] Peppas NA, Keys KB, Torres-Lugo M, Lowman AM. Poly(ethylene glycol)-containing hydrogels in drug delivery. J Controlled Release 1999;62(1–2):81–7. http://dx.doi.org/10.1016/S0168-3659(99)00027-9.

[5] Peppas NA, Hilt JZ, Khademhosseini A, Langer R. Hydrogels in biology and medicine: from molecular principles to bionanotechnology. Adv Mater 2006;18(11):1345–60. http://dx.doi.org/10.1002/adma.200501612.

[6] Lee KY, Mooney DJ. Hydrogels for tissue engineering. Chem Rev 2001;101(7):1869–79. http://dx.doi.org/10.1021/cr000108x.

[7] Nguyen KT, West JL. Photopolymerizable hydrogels for tissue engineering applications. Biomaterials 2002;23(22):4307–14. http://dx.doi.org/10.1016/S0142-9612(02)00175-8.

[8] Slaughter BV, Khurshid SS, Fisher OZ, Khademhosseini A, Peppas NA. Hydrogels in regenerative medicine. Adv Mater 2009;21(32–33):3307–29. http://dx.doi.org/10.1002/adma.200802106.

[9] Eddington DT, Beebe DJ. Flow control with hydrogels. Adv Drug Deliv Rev 2004;56(2):199–210. http://dx.doi.org/10.1016/j.addr.2003.08.013.

[10] Burdick JA, Murphy WL. Moving from static to dynamic complexity in hydrogel design. Nat Commun 2012;3:1269. http://dx.doi.org/10.1038/ncomms2271.

[11] Whitesides GM, Stroock AD. Flexible methods for microfluidics. Phys Today 2001;54(6):42–8. http://dx.doi.org/10.1063/1.1387591.

[12] Gates BD, Xu Q, Stewart M, Ryan D, Willson CG, Whitesides GM. New approaches to nanofabrication: molding, printing, and other techniques. Chem Rev 2005;105(4):1171–96. http://dx.doi.org/10.1021/cr030076o.

[13] Casadevall i Solvas X, deMello A. Droplet microfluidics: recent developments and future applications. Chem Commun 2011;47(7):1936–42. http://dx.doi.org/10.1039/C0CC02474.

[14] Kumacheva E, Garstecki P. Synthesis of polymer particles in microfluidic reactors. Microfluidic reactors for polymer particles. John Wiley & Sons, Ltd; 2011. p. 109–45.

[15] Buenger D, Topuz F, Groll J. Hydrogels in sensing applications. Prog Polym Sci 2012;37(12):1678–719. http://dx.doi.org/10.1016/j.progpolymsci.2012.09.001.

[16] Neumann T, Bonham AJ, Dame G, Berchtold B, Brandstetter T, Rühe Jr. Temperature and time-resolved total internal reflectance fluorescence analysis of reusable DNA hydrogel chips. Anal Chem 2010;82(14):6124–31. http://dx.doi.org/10.1021/ac1008578.

[17] Le Goff GC, Blum LJ, Marquette CA. Shrinking hydrogel-DNA spots generates 3D microdots arrays. Macromol Biosci 2013;13(2):227–33. http://dx.doi.org/10.1002/mabi.201200370.

[18] Lee A, Beebe D, Palecek S. Quantification of kinase activity in cell lysates via photopatterned macroporous poly(ethylene glycol) hydrogel arrays in microfluidic channels. Biomed Microdev 2012;14(2):247–57. http://dx.doi.org/10.1007/s10544-011-9602-y.

[19] Lin Z, Ma Y, Zhao C, Chen R, Zhu X, Zhang L, et al. An extremely simple method for fabricating 3D protein microarrays with an anti-fouling background and high protein capacity. Lab Chip 2014. http://dx.doi.org/10.1039/c4lc00223g.

[20] Lee AG, Arena CP, Beebe DJ, Palecek SP. Development of macroporous poly(ethylene glycol) hydrogel arrays within microfluidic channels. Biomacromolecules 2010;11(12):3316–24. http://dx.doi.org/10.1021/bm100792y.

[21] Li H, Leulmi RF, Juncker D. Hydrogel droplet microarrays with trapped antibody-functionalized beads for multiplexed protein analysis. Lab Chip 2011;11(3):528–34. http://dx.doi.org/10.1039/c0lc00291g.

[22] Proudnikov D, Timofeev E, Mirzabekov A. Immobilization of DNA in polyacrylamide gel for the manufacture of DNA and DNA-oligonucleotide microchips. Anal Biochem 1998;259(1):34–41. http://dx.doi.org/10.1006/abio.1998.2620.

[23] Fotin AV, Drobyshev AL, Proudnikov DY, Perov AN, Mirzabekov AD. Parallel thermodynamic analysis of duplexes on oligodeoxyribonucleotide microchips. Nucleic Acids Res 1998;26(6):1515–21. http://dx.doi.org/10.1093/Nar/26.6.1515.

[24] Kolchinsky AM, Gryadunov DA, Lysov YP, Mikhailovich VM, Nasedkina TV, Turygin AY, et al. Gel-based microchips: history and prospects. Mol Biol 2004;38(1):4–13. http://dx.doi.org/10.1023/B:Mbil. 0000015134.67385.Fd.

[25] Sorokin NV, Chechetkin VR, Pan'kov SV, Somova OG, Livshits MA, Donnikov MY, et al. Kinetics of hybridization on surface oligonucleotide microchips: theory, experiment, and comparison with hybridization on gel-based microchips. J Biomol Struct Dyn 2006;24(1):57–66. http://dx.doi.org/10.1080/07391102.2006.10507099.

[26] Zubtsov DA, Savvateeva EN, Rubina AY, Pan'kov SV, Konovalova EV, Moiseeva OV, et al. Comparison of surface and hydrogel-based protein microchips. Anal Biochem 2007;368(2):205–13. http://dx.doi.org/10.1016/j.ab.2007.04.040.

[27] Arenkov P, Kukhtin A, Gemmell A, Voloshchuk S, Chupeeva V, Mirzabekov A. Protein microchips: use for immunoassay and enzymatic reactions. Anal Biochem 2000;278(2):123–31. http://dx.doi.org/10.1006/Abio.1999.4363.

[28] Squires TM, Messinger RJ, Manalis SR. Making it stick: convection, reaction and diffusion in surface-based biosensors. Nat Biotechnol 2008;26(4):417–26. http://dx.doi.org/10.1038/nbt1388.

[29] Birtwell S, Morgan H. Microparticle encoding technologies for high-throughput multiplexed suspension assays. Integr Biol 2009;1(5–6):345–62. http://dx.doi.org/10.1039/B905502a.

[30] Guo MT, Rotem A, Heyman JA, Weitz DA. Droplet microfluidics for high-throughput biological assays. Lab Chip 2012;12(12):2146–55. http://dx.doi.org/10.1039/C2LC21147E.

[31] Seiffert S. Microgel capsules tailored by droplet-based microfluidics. ChemPhysChem 2013;14(2):295–304. http://dx.doi.org/10.1002/cphc.201200749.

[32] Hucknall A, Rangarajan S, Chilkoti A. In pursuit of zero: polymer brushes that resist the adsorption of proteins. Adv Mater 2009;21(23):2441–6. http://dx.doi.org/10.1002/adma.200900383.

[33] Meiring JE, Schmid MJ, Grayson SM, Rathsack BM, Johnson DM, Kirby R, et al. Hydrogel biosensor array platform indexed by shape. Chem Mater 2004;16(26):5574–80. http://dx.doi.org/10.1021/cm049488j.

[34] Choi D, Jang E, Park J, Koh WG. Development of microfluidic devices incorporating non-spherical hydrogel microparticles for protein-based bioassay. Microfluid Nanofluid 2008;5(5):703–10. http://dx.doi.org/10.1007/s10404-008-0303-7.

[35] Pregibon DC, Doyle PS. Optimization of encoded hydrogel particles for nucleic acid quantification. Anal Chem 2009;81(12):4873–81. http://dx.doi.org/10.1021/Ac9005292.

[36] Park S, Lee Y, Kim DN, Jang E, Koh WG. Entrapment of enzyme-linked magnetic nanoparticles within poly(ethylene glycol) hydrogel microparticles prepared by photopatterning. React Funct

Polym 2009;69(5):293–9. http://dx.doi.org/10.1016/j.reactfunctpolym.2009.02.001.

[37] Lewis CL, Choi CH, Lin Y, Lee CS, Yi H. Fabrication of uniform DNA-conjugated hydrogel microparticles via replica molding for facile nucleic acid hybridization assays. Anal Chem 2010;82(13):5851–8. http://dx.doi.org/10.1021/ac101032r.

[38] Lee H, Kim J, Kim H, Kwon S. Colour-barcoded magnetic microparticles for multiplexed bioassays. Nat Mater 2010;9(9):745–9. http://dx.doi.org/10.1038/nmat2815.

[39] Kantak C, Zhu QD, Beyer S, Bansal T, Trau D. Utilizing microfluidics to synthesize polyethylene glycol microbeads for Forster resonance energy transfer based glucose sensing. Biomicrofluidics 2012;6(2). http://dx.doi.org/10.1063/1.369486.

[40] Gerver RE, Gomez-Sjoberg R, Baxter BC, Thorn KS, Fordyce PM, Diaz-Botia CA, et al. Programmable microfluidic synthesis of spectrally encoded microspheres. Lab Chip 2012;12(22):4716–23. http://dx.doi.org/10.1039/C2LC40699C.

[41] Andrzejewska E. Photopolymerization kinetics of multifunctional monomers. Prog Polym Sci 2001;26(4):605–65. http://dx.doi.org/10.1016/S0079-6700(01)00004-1.

[42] Park S, Kim D, Ko SY, Park J-O, Akella S, Xu B, et al. Controlling uniformity of photopolymerized microscopic hydrogels. Lab Chip 2014. http://dx.doi.org/10.1039/c4lc00158c.

[43] Dendukuri D, Panda P, Haghgooie R, Kim JM, Hatton TA, Doyle PS. Modeling of oxygen-inhibited free radical photopolymerization in a PDMS microfluidic device. Macromolecules 2008;41(22):8547–56. http://dx.doi.org/10.1021/Ma801219w.

[44] Chapin SC, Pregibon DC, Doyle PS. High-throughput flow alignment of barcoded hydrogel microparticles. Lab Chip 2009;9(21):3100–9. http://dx.doi.org/10.1039/b909959j.

[45] Choi NW, Kim J, Chapin SC, Duong T, Donohue E, Pandey P, et al. Multiplexed detection of mRNA using porosity-tuned hydrogel microparticles. Anal Chem 2012;84(21):9370–8. http://dx.doi.org/10.1021/ac302128u.

[46] Wu Y-H, Park HB, Kai T, Freeman BD, Kalika DS. Water uptake, transport and structure characterization in poly(ethylene glycol) diacrylate hydrogels. J Membr Sci 2010;347(1–2):197–208. http://dx.doi.org/10.1016/j.memsci.2009.10.025.

[47] Hwang DK, Oakey J, Toner M, Arthur JA, Anseth KS, Lee S, et al. Stop-flow lithography for the production of shape-evolving degradable microgel particles. J Am Chem Soc 2009;131(12):4499–504. http://dx.doi.org/10.1021/Ja809256d.

[48] Jung S, Yi H. Fabrication of chitosan-poly(ethylene glycol) hybrid hydrogel microparticles via replica molding and its application toward facile conjugation of biomolecules. Langmuir 2012. http://dx.doi.org/10.1021/la303567p.

[49] Jung S, Yi H. Facile strategy for protein conjugation with chitosan-poly(ethylene glycol) hybrid microparticle platforms via strain-promoted alkyne-azide cycloaddition (SPAAC) reaction. Biomacromolecules 2013;14(11):3892–902. http://dx.doi.org/10.1021/bm401018h.

[50] Ye B-F, Zhao Y-J, Li T-T, Xie Z-Y, Gu Z-Z. Aptamer-based suspension array indexed by structural color and shape. J Mater Chem 2011;21(46):18659–64. http://dx.doi.org/10.1039/C1JM14009D.

[51] Appleyard DC, Chapin SC, Srinivas RL, Doyle PS. Bar-coded hydrogel microparticles for protein detection: synthesis, assay and scanning. Nat Protocols 2011;6(11):1761–74. http://dx.doi.org/10.1038/nprot.2011.400.

[52] Yi HM, Wu LQ, Bentley WE, Ghodssi R, Rubloff GW, Culver JN, et al. Biofabrication with chitosan. Biomacromolecules 2005;6(6):2881–94. http://dx.doi.org/10.1021/bm0504101.

[53] Ji X-H, Zhang N-G, Cheng W, Guo F, Liu W, Guo S-S, et al. Integrated parallel microfluidic device for simultaneous preparation of multiplex optical-encoded microbeads with distinct quantum dot barcodes. J Mater Chem 2011;21(35):13380–7. http://dx.doi.org/10.1039/C1JM12253C.

[54] Maeda K, Onoe H, Takinoue M, Takeuchi S. Controlled synthesis of 3D multi-compartmental particles with centrifuge-based microdroplet formation from a multi-barrelled capillary. Adv Mater 2012;24(10):1340–6. http://dx.doi.org/10.1002/adma.201102560.

[55] Lee J, Kim J. Multiphasic sensory alginate particle having polydiacetylene liposome for selective and more sensitive multitargeting detection. Chem Mater 2012;24(14):2817–22. http://dx.doi.org/10.1021/Cm3015012.

[56] Lee KY, Mooney DJ. Alginate: properties and biomedical applications. Prog Polym Sci 2012;37(1):106–26. http://dx.doi.org/10.1016/j.progpolymsci.2011.06.003.

[57] Augst AD, Kong HJ, Mooney DJ. Alginate hydrogels as biomaterials. Macromol Biosci 2006;6(8):623–33. http://dx.doi.org/10.1002/mabi.200600069.

[58] Pawar SN, Edgar KJ. Alginate derivatization: a review of chemistry, properties and applications. Biomaterials 2012;33(11):3279–305. http://dx.doi.org/10.1016/j.biomaterials.2012.01.007.

[59] Khademhosseini A, Langer R. Microengineered hydrogels for tissue engineering. Biomaterials 2007;28(34):5087–92. http://dx.doi.org/10.1016/j.biomaterials.2007.07.021.

[60] Oh JK, Drumright R, Siegwart DJ, Matyjaszewski K. The development of microgels/nanogels for drug delivery applications. Prog Polym Sci 2008;33(4):448–77. http://dx.doi.org/10.1016/j.progpolymsci.2008.01.002.

[61] Matricardi P, Di Meo C, Coviello T, Alhaique F. Recent advances and perspectives on coated alginate microspheres for modified drug delivery. Exp Opin Drug Deliv 2008;5(4):417–25. http://dx.doi.org/10.1517/17425247.5.4.417.

[62] Tan WH, Takeuchi S. Monodisperse alginate hydrogel microbeads for cell encapsulation. Adv Mater 2007;19(18):2696–701. http://dx.doi.org/10.1002/adma.200700433.

[63] Martinez CJ, Kim JW, Ye C, Ortiz I, Rowat AC, Marquez M, et al. A microfluidic approach to encapsulate living cells in uniform alginate hydrogel microparticles. Macromol Biosci 2012;12(7):946–51. http://dx.doi.org/10.1002/mabi.201100351.

[64] Thomas S. Alginate dressings in surgery and wound management – Part 1. J Wound Care 2000;9(2):56–60. http://dx.doi.org/10.12968/jowc.2000.9.2.26338.

[65] Ji X-H, Cheng W, Guo F, Liu W, Guo S-S, He Z-K, et al. On-demand preparation of quantum dot-encoded microparticles using a droplet microfluidic system. Lab Chip 2011;11(15):2561–8. http://dx.doi.org/10.1039/C1LC20150F.

[66] Zhu Q, Trau D. Multiplex detection platform for tumor markers and glucose in serum based on a microfluidic microparticle array. Anal Chim Acta 2012;751:146–54. http://dx.doi.org/10.1016/j.aca.2012.09.007.

[67] Lee W, Choi D, Kim JH, Koh WG. Suspension arrays of hydrogel microparticles prepared by photopatterning for multiplexed protein-based bioassays. Biomed Microdev 2008;10(6):813–22. http://dx.doi.org/10.1007/s10544-008-9196-1.

[68] Bong KW, Chapin SC, Doyle PS. Magnetic barcoded hydrogel microparticles for multiplexed detection. Langmuir 2010;26(11):8008–14. http://dx.doi.org/10.1021/la904903g.

[69] Pregibon DC, Toner M, Doyle PS. Multifunctional encoded particles for high-throughput biomolecule analysis. Science 2007;315(5817):1393–6. http://dx.doi.org/10.1126/science.1134929.

[70] Chapin SC, Appleyard DC, Pregibon DC, Doyle PS. Rapid microRNA profiling on encoded gel microparticles. Angew Chem Int Ed 2011;50(10):2289–93. http://dx.doi.org/10.1002/anie.201006523.

[71] Srinivas RL, Chapin SC, Doyle PS. Aptamer-functionalized microgel particles for protein detection. Anal Chem 2011;83(23):9138–45. http://dx.doi.org/10.1021/ac202335u.

[72] Appleyard DC, Chapin SC, Doyle PS. Multiplexed protein quantification with barcoded hydrogel microparticles. Anal Chem 2011;83(1):193–9. http://dx.doi.org/10.1021/Ac1022343.

[73] Salinas CN, Anseth KS. Mixed mode thiol–acrylate photopolymerizations for the synthesis of PEG–peptide hydrogels. Macromolecules 2008;41(16):6019–26. http://dx.doi.org/10.1021/ma800621h.

[74] Park S, Lee HJ, Koh WG. Multiplex immunoassay platforms based on shape-coded poly(ethylene glycol) hydrogel microparticles incorporating acrylic acid. Sensors-Basel 2012;12(6):8426–36. http://dx.doi.org/10.3390/S120608426.

[75] He M, Herr AE. Automated microfluidic protein immunoblotting. Nat Protocols 2010;5(11):1844–56. http://dx.doi.org/10.1038/nprot.2010.142.

[76] Jung S, Yi HM. An integrated approach for enhanced protein conjugation and capture with viral nanotemplates and hydrogel microparticle platforms via rapid bioorthogonal reactions. Langmuir 2014;30(26):7762–70. http://dx.doi.org/10.1021/la501772t.

[77] Sorokin NV, Chechetkin VR, Livshits MA, Pan'kov SV, Donnikov MY, Gryadunov DA, et al. Discrimination between perfect and mismatched duplexes with oligonucleotide gel microchips: role of thermodynamic and kinetic effects during hybridization. J Biomol Struct Dyn 2005;22(6):725–34. http://dx.doi.org/10.1080/07391102.2005.10507039.

[78] Levicky R, Horgan A. Physicochemical perspectives on DNA microarray and biosensor technologies. Trends Biotechnol 2005;23(3):143–9. http://dx.doi.org/10.1016/j.tibtech.2005.01.004.

[79] Kumacheva E, Garstecki P. Methods for the generation of polymer particles. Microfluidic reactors for polymer particles. John Wiley & Sons, Ltd; 2011. p. 7–15.

[80] Sun X-T, Liu M, Xu Z-R. Microfluidic fabrication of multifunctional particles and their analytical applications. Talanta 2014;121:163–77. http://dx.doi.org/10.1016/j.talanta.2013.12.060.

[81] Lee J, Bisso PW, Srinivas RL, Kim JJ, Swiston AJ, Doyle PS. Universal process-inert encoding architecture for polymer microparticles. Nat Mater 2014;13(5):524–9. http://dx.doi.org/10.1038/nmat3938.

[82] Lim CT, Zhang Y. Bead-based microfluidic immunoassays: the next generation. Biosens Bioelectron 2007;22(7):1197–204. http://dx.doi.org/10.1016/j.bios.2006.06.005.

[83] Cederquist KB, Dean SL, Keating CD. Encoded anisotropic particles for multiplexed bioanalysis. WIREs Nanomed Nanobiotechnol 2010;2(6):578–600. http://dx.doi.org/10.1002/Wnan.96.

[84] Luminex Corporation. Technologies & Science; <http://www.luminexcorp.com/TechnologiesScience/> [accessed 15.12.14].

[85] BD Biosciences. Bead-based immunoassays; <http://www.bdbiosciences.com/research/cytometricbeadarray/index.jsp> [accessed 15.12.14].

[86] Jang E, Park S, Park S, Lee Y, Kim D-N, Kim B, et al. Fabrication of poly(ethylene glycol)-based hydrogels entrapping enzyme-immobilized silica nanoparticles. Polym Adv Technol 2010;21(7):476–82. http://dx.doi.org/10.1002/pat.1455.

[87] Du YA, Lo E, Ali S, Khademhosseini A. Directed assembly of cell-laden microgels for fabrication of 3D tissue constructs. Proc Natl Acad Sci USA 2008;105(28):9522–7. http://dx.doi.org/10.1073/pnas.0801866105.

[88] Dendukuri D, Pregibon DC, Collins J, Hatton TA, Doyle PS. Continuous-flow lithography for high-throughput microparticle synthesis. Nat Mater 2006;5(5):365–9. http://dx.doi.org/10.1038/nmat1617.

[89] Dendukuri D, Gu SS, Pregibon DC, Hatton TA, Doyle PS. Stop-flow lithography in a microfluidic device. Lab Chip 2007;7(7):818–28. http://dx.doi.org/10.1039/B703457a.

[90] Doyle PS, Pregibon DC, Dendukuri D. Microstructure synthesis by flow lithography and polymerization; 2010. US7709544 (B2).

[91] Bong KW, Chapin SC, Pregibon DC, Baah D, Floyd-Smith TM, Doyle PS. Compressed-air flow control system. Lab Chip 2011;11(4):743–7. http://dx.doi.org/10.1039/C0lc00303d.

[92] Chapin SC, Doyle PS. Ultrasensitive multiplexed microRNA quantification on encoded gel microparticles using rolling circle amplification. Anal Chem 2011;83(18):7179–85. http://dx.doi.org/10.1021/Ac201618k.

[93] Bong KW, Bong KT, Pregibon DC, Doyle PS. Hydrodynamic focusing lithography. Angew Chem Int Ed 2010;49(1):87–90. http://dx.doi.org/10.1002/anie.200905229.

[94] Bong KW, Xu J, Kim J-H, Chapin SC, Strano MS, Gleason KK, et al. Non-polydimethylsiloxane devices for oxygen-free flow lithography. Nat Commun 2012;3. http://dx.doi.org/10.1038/ncomms180.

[95] An HZ, Safai ER, Eral HB, Doyle PS. Synthesis of biomimetic oxygen-carrying compartmentalized microparticles using flow lithography. Lab Chip 2013;13(24):4765–74. http://dx.doi.org/10.1039/C3lc50610j.

[96] Hakimi N, Tsai SSH, Cheng C-H, Hwang DK. One-step two-dimensional microfluidics-based synthesis of three-dimensional particles. Adv Mater 2014;26(9):1393–8. http://dx.doi.org/10.1002/adma.201304378.

[97] Kim LN, Choi S-E, Kim J, Kim H, Kwon S. Single exposure fabrication and manipulation of 3D hydrogel cell microcarriers. Lab Chip 2011;11(1):48–51. http://dx.doi.org/10.1039/C1JM12253C.

[98] Chung SE, Park W, Park H, Yu K, Park N, Kwon S. Optofluidic maskless lithography system for real-time synthesis of photopolymerized microstructures in microfluidic channels. Appl Phys Lett 2007;91(4). http://dx.doi.org/10.1063/1.275998.

[99] Rolland JP, Maynor BW, Euliss LE, Exner AE, Denison GM, DeSimone JM. Direct fabrication and harvesting of monodisperse, shape-specific nanobiomaterials. J Am Chem Soc 2005;127(28):10096–100. http://dx.doi.org/10.1021/ja051977c.

[100] Galloway A, Murphy A, Rolland J, Herlihy K, Petros R, Napier M, et al. Micromolding for the fabrication of biological microarrays. In: Khademhosseini A, Suh K-Y, Zourob M, editors. Biological microarrays. Humana Press; 2011. p. 249–60.

[101] Perry JL, Herlihy KP, Napier ME, DeSimone JM. PRINT: a novel platform toward shape and size specific nanoparticle theranostics. Acc Chem Res 2011;44(10):990–8. http://dx.doi.org/10.1021/ar2000315.

[102] Dendukuri D, Doyle PS. The synthesis and assembly of polymeric microparticles using microfluidics. Adv Mater 2009;21(41):4071–86. http://dx.doi.org/10.1038/nmat1617.

[103] Wang J-T, Wang J, Han J-J. Fabrication of advanced particles and particle-based materials assisted by droplet-based microfluidics. Small 2011;7(13):1728–54. http://dx.doi.org/10.1002/smll.201001913.

[104] Yang S, Guo F, Kiraly B, Mao X, Lu M, Leong KW, et al. Microfluidic synthesis of multifunctional Janus particles for biomedical applications. Lab Chip 2012;12(12):2097–102. http://dx.doi.org/10.1039/C2LC90046G.

[105] Desmarais SM, Haagsman HP, Barron AE. Microfabricated devices for biomolecule encapsulation. Electrophoresis 2012;33(17):2639–49. http://dx.doi.org/10.1002/elps.201200189.

[106] Zhao Y, Cheng Y, Shang L, Wang J, Xie Z, Gu Z. Microfluidic synthesis of barcode particles for multiplex assays. Small 2014. http://dx.doi.org/10.1002/smll.20140160.

[107] Hu J, Zhao XW, Zhao YJ, Li J, Xu WY, Wen ZY, et al. Photonic crystal hydrogel beads used for multiplex biomolecular detection. J Mater Chem 2009;19(32):5730–6. http://dx.doi.org/10.1039/b906652g.

[108] Zhao YJ, Zhao XW, Tang BC, Xu WY, Gu ZZ. Rapid and sensitive biomolecular screening with encoded macroporous hydrogel photonic beads. Langmuir 2010;26(9):6111–4. http://dx.doi.org/10.1021/La100939d.

[109] Um E, Lee DS, Pyo HB, Park JK. Continuous generation of hydrogel beads and encapsulation of biological materials using a microfluidic droplet-merging channel. Microfluid Nanofluid 2008;5(4):541–9. http://dx.doi.org/10.1007/S10404-008-0268-6.

[110] Zhao Y, Shum HC, Chen H, Adams LLA, Gu Z, Weitz DA. Microfluidic generation of multifunctional quantum dot barcode particles. J Am Chem Soc 2011;133(23):8790–3. http://dx.doi.org/10.1021/ja200729w.

[111] Cheng Y, Zhu C, Xie Z, Gu H, Tian T, Zhao Y, et al. Anisotropic colloidal crystal particles from microfluidics. J Colloid Interface Sci 2014;421:64–70. http://dx.doi.org/10.1016/j.jcis.2014.01.041.

[112] Derveaux S, Stubbe B, Braeckmans K, Roelant C, Sato K, Demeester J, et al. Synergism between particle-based multiplexing and microfluidics technologies may bring diagnostics closer to the patient. Anal Bioanal Chem 2008;391(7):2453–67. http://dx.doi.org/10.1007/s00216-008-2062-4.

[113] Eng G, Lee BW, Parsa H, Chin CD, Schneider J, Linkov G, et al. Assembly of complex cell microenvironments using geometrically docked hydrogel shapes. Proc Natl Acad Sci USA 2013;110(12):4551–6. http://dx.doi.org/10.1073/pnas.1300569110.

[114] Eun Chung S, Kim J, Yoon Oh D, Song Y, Hoon Lee S, Min S, et al. One-step pipetting and assembly of encoded chemical-laden microparticles for high-throughput multiplexed bioassays. Nat Commun 2014;5. http://dx.doi.org/10.1038/ncomms446.

[115] Suh S, Chapin S, Hatton TA, Doyle P. Synthesis of magnetic hydrogel microparticles for bioassays and tweezer manipulation in microwells. Microfluid Nanofluid 2012:1–10. http://dx.doi.org/10.1007/s10404-012-0977-.

[116] Wilson R, Cossins AR, Spiller DG. Encoded microcarriers for high-throughput multiplexed detection. Angew Chem Int Ed 2006;45(37):6104–17. http://dx.doi.org/10.1002/anie.200600288.

[117] Birtwell SW, Broder GR, Roach PL, Morgan H. Multiplexed suspension array platform for high-throughput protein assays. Biomed Microdev 2012;14(4):651–7. http://dx.doi.org/10.1007/s10544-012-9641-z.

[118] Lewis CL, Lin Y, Yang CX, Manocchi AK, Yuet KP, Doyle PS, et al. Microfluidic fabrication of hydrogel microparticles containing functionalized viral nanotemplates. Langmuir 2010;26(16):13436–41. http://dx.doi.org/10.1021/La1044611.

[119] Meiring JE, Lee S, Costner EA, Schmid MJ, Michaelson TB, Willson CG, et al. Pattern recognition of shape-encoded hydrogel biosensor arrays. Opt Eng 2009;48(3). http://dx.doi.org/10.1117/1.309972.

[120] Firefly Bioworks Technology; <http://www.fireflybio.com/technology> [accessed 15.12.14].

[121] Tumarkin E, Tzadu L, Csaszar E, Seo M, Zhang H, Lee A, et al. High-throughput combinatorial cell co-culture using microfluidics. Integr Biol 2011;3(6):653–62. http://dx.doi.org/10.1039/c1ib00002k.

[122] Zhao YJ, Zhao XW, Tang BC, Xu WY, Li J, Hu L, et al. Quantum-dot-tagged bioresponsive hydrogel suspension array for multiplex label-free DNA detection. Adv Funct Mater 2010;20(6):976–82. http://dx.doi.org/10.1002/adfm.200901812.

[123] Zhang HB, DeConinck AJ, Slimmer SC, Doyle PS, Lewis JA, Nuzzo RG. Genotyping by alkaline dehybridization using graphically encoded

particles. Chem – Eur J 2011;17(10):2867–73. http://dx.doi.org/10.1002/chem.201002848.

[124] Yang Z-X, Chen B-A, Wang H, Xia G-H, Cheng J, Pei X-P, et al. Handy, rapid and multiplex detection of tumor markers based on encoded silica–hydrogel hybrid beads array chip. Biosens Bioelectron 2013;48:153–7. http://dx.doi.org/10.1016/j.bios.2013.04.014.

[125] Cho EJ, Lee J-W, Ellington AD. Applications of aptamers as sensors. Annu Rev Anal Chem 2009;2(1):241–64. http://dx.doi.org/10.1146/annurev.anchem.1.031207.112851.

[126] Sandhu SK, Fassan M, Volinia S, Lovat F, Balatti V, Pekarsky Y, et al. B-cell malignancies in microRNA Eμ-miR-17–92 transgenic mice. Proc Natl Acad Sci USA 2013;110(45):18208–13. http://dx.doi.org/10.1073/pnas.1315365110.

[127] Zhao Y-J, Zhao X-W, Hu J, Li J, Xu W-Y, Gu Z-Z. Multiplex label-free detection of biomolecules with an imprinted suspension array. Angew Chem Int Ed 2009;48(40):7350–2. http://dx.doi.org/10.1002/anie.200903472.

[128] Doring A, Birnbaum W, Kuckling D. Responsive hydrogels – structurally and dimensionally optimized smart frameworks for applications in catalysis, micro-system technology and material science. Chem Soc Rev 2013. http://dx.doi.org/10.1039/c3cs60031a.

[129] Pinaud F, Russo L, Pinet S, Gosse I, Ravaine V, Sojic N. Enhanced electrogenerated chemiluminescence in thermoresponsive microgels. J Am Chem Soc 2013;135(15):5517–20. http://dx.doi.org/10.1021/ja401011j.

[130] Kim JS, Singh N, Lyon LA. Label-free biosensing with hydrogel microlenses. Angew Chem Int Ed 2006;45(9):1446–9. http://dx.doi.org/10.1002/anie.200503102.

[131] Huang SH, Lin CK. Stop-flow lithography to continuously fabricate microlens structures utilizing an adjustable three-dimensional mask. Micromachines 2014;5(3):667–80. http://dx.doi.org/10.3390/mi5030667.

[132] Longo C, Patanarut A, George T, Bishop B, Zhou W, Fredolini C, et al. Core–shell hydrogel particles harvest, concentrate and preserve labile low abundance biomarkers. PLOS ONE 2009;4(3):e4763. http://dx.doi.org/10.1371/journal.pone.0004763.

[133] Douglas TA, Tamburro D, Fredolini C, Espina BH, Lepene BS, Ilag L, et al. The use of hydrogel microparticles to sequester and concentrate bacterial antigens in a urine test for Lyme disease. Biomaterials 2011;32(4):1157–66. http://dx.doi.org/10.1016/j.biomaterials.2010.10.004.

[134] Thermo Fisher Scientific Inc. Pull down assays; <http://www.piercenet.com/method/pull-down-assays> [accessed 15.12.14].

[135] Zhang L, Lei J, Liu L, Li C, Ju H. Self-assembled DNA hydrogel as switchable material for aptamer-based fluorescent detection of protein. Anal Chem 2013. http://dx.doi.org/10.1021/ac4027725.

[136] Wang R, Li Y. Hydrogel based QCM aptasensor for detection of avian influenza virus. Biosens Bioelectron 2013;42:148–55. http://dx.doi.org/10.1016/j.bios.2012.10.038.

[137] Wang D, Bodovitz S. Single cell analysis: the new frontier in 'omics'. Trends Biotechnol 2010;28(6):281–90. http://dx.doi.org/10.1016/j.tibtech.2010.03.002.

[138] Zare R, Kim S. Microfluidic platforms for single-cell analysis. Annu Rev Biomed Eng 2010;12:187–201.

[139] Joensson HN, Andersson Svahn H. Droplet microfluidics—a tool for single-cell analysis. Angew Chem Int Ed 2012;51(49):12176–92. http://dx.doi.org/10.1002/anie.20120046.

[140] Han Q, Bradshaw E, Nilsson B, Hafler D, Love JC. Multidimensional analysis of the frequencies and rates of cytokine secretion from single cells by quantitative microengraving. Lab Chip 2010;10(11):1391–400. http://dx.doi.org/10.1039/B926849A.

[141] Fluidigm. Products – C1 system; <https://www.fluidigm.com/products/c1-system> [accessed 15.12.14].

[142] Ma C, Fan R, Ahmad H, Shi Q, Comin-Anduix B, Chodon T, et al. A clinical microchip for evaluation of single immune cells reveals high functional heterogeneity in phenotypically similar T cells. Nat Med 2011;17(6):738–43. http://dx.doi.org/10.1038/nm.2375.

[143] Tibbitt MW, Anseth KS. Hydrogels as extracellular matrix mimics for 3D cell culture. Biotechnol Bioeng 2009;103(4):655–63. http://dx.doi.org/10.1002/bit.22361.

[144] Chung BG, Lee K-H, Khademhosseini A, Lee S-H. Microfluidic fabrication of microengineered hydrogels and their application in tissue engineering. Lab Chip 2012;12(1):45–59. http://dx.doi.org/10.1039/C1LC20859D.

[145] Velasco D, Tumarkin E, Kumacheva E. Microfluidic encapsulation of cells in polymer microgels. Small 2012;8(11):1633–42. http://dx.doi.org/10.1002/smll.201102464.

[146] Li C, Stevens K, Schwartz R, Alejandro B, Huang J, Bhatia S. Micropatterned cell–cell interactions enable functional encapsulation of primary hepatocytes in hydrogel microtissues. Tissue Eng Part A 2014;20(15–16):2200–12. http://dx.doi.org/10.1089/ten.tea.2013.0667.

[147] Kumachev A, Greener J, Tumarkin E, Eiser E, Zandstra PW, Kumacheva E. High-throughput generation of hydrogel microbeads with varying elasticity for cell encapsulation. Biomaterials 2011;32(6):1477–83. http://dx.doi.org/10.1016/j.biomaterials.2010.10.033.

[148] Wan J. Microfluidic-based synthesis of hydrogel particles for cell microencapsulation and cell-based drug delivery. Polymers 2012;4(2):1084–108. http://dx.doi.org/10.3390/polym4021084.

[149] Aikawa T, Konno T, Takai M, Ishihara K. Spherical phospholipid polymer hydrogels for cell encapsulation prepared with a flow-focusing microfluidic channel device. Langmuir 2012;28(4):2145–50. http://dx.doi.org/10.1021/la2037586.

[150] Panda P, Ali S, Lo E, Chung B, Hatton TA, Khademhosseini A, et al. Stop-flow lithography to generate cell-laden microgel particles. Lab Chip 2008;8(7):1056–61. http://dx.doi.org/10.1039/b804234a.